Abscisic Acid Flux Alterations Result in Differential Abscisic Acid Signaling Responses and Impact Assimilation Efficiency in Barley under Terminal Drought Stress[1][C][W][OPEN]

Christiane Seiler[2], Vokkaliga T. Harshavardhan[2], Palakolanu Sudhakar Reddy, Götz Hensel, Jochen Kumlehn, Lennart Eschen-Lippold, Kalladan Rajesh, Viktor Korzun, Ulrich Wobus, Justin Lee, Gopalan Selvaraj, and Nese Sreenivasulu[3]*

Leibniz Institute of Plant Genetics and Crop Plant Research, D–06466 Gatersleben, Germany (C.S., V.T.H., P.S.R., G.H., J.K., K.R., U.W., N.S.); Leibniz Institute of Plant Biochemistry, D–06120 Halle, Germany (L.E.-L., J.L.); Kleinwanzlebener Saatzucht KWS LOCHOW GmbH, D–29303 Bergen, Germany (V.K.); National Research Council of Canada, Saskatoon, Canada S7N 0W9 (G.S.); and Research Group Abiotic Stress Genomics, Interdisciplinary Center for Crop Plant Research, D–06120 Halle, Germany (N.S.)

ORCID ID: 0000-0002-3998-038X (N.S.).

Abscisic acid (ABA) is a central player in plant responses to drought stress. How variable levels of ABA under short-term versus long-term drought stress impact assimilation and growth in crops is unclear. We addressed this through comparative analysis, using two elite breeding lines of barley (*Hordeum vulgare*) that show senescence or stay-green phenotype under terminal drought stress and by making use of transgenic barley lines that express Arabidopsis (*Arabidopsis thaliana*) 9-cis-epoxycarotenoid dioxygenase (*AtNCED6*) coding sequence or an RNA interference (RNAi) sequence of ABA 8′-hydroxylase under the control of a drought-inducible barley promoter. The high levels of ABA and its catabolites in the senescing breeding line under long-term stress were detrimental for assimilate productivity, whereas these levels were not perturbed in the stay-green type that performed better. In transgenic barley, drought-inducible *AtNCED* expression afforded temporal control in ABA levels such that the ABA levels rose sooner than in wild-type plants but also subsided, unlike as in the wild type , to near-basal levels upon prolonged stress treatment due to down-regulation of endogenous *HvNCED* genes. Suppressing of ABA catabolism with the RNA interference approach of ABA 8′-hydroxylase caused ABA flux during the entire period of stress. These transgenic plants performed better than the wild type under stress to maintain a favorable instantaneous water use efficiency and better assimilation. Gene expression analysis, protein structural modeling, and protein-protein interaction analyses of the members of the *PYRABACTIN RESISTANCE1/PYRABACTIN RESISTANCE1-LIKE/REGULATORY COMPONENT OF ABA RECEPTORS*, *TYPE 2C PROTEIN PHOSPHATASE Sucrose non-fermenting1-related protein kinase2*, and *ABA-INSENSITIVE5/ABA-responsive element binding factor* family identified specific members that could potentially impact ABA metabolism and stress adaptation in barley.

Drought compromises grain yield in cereals, especially when the stress occurs during postanthesis (Boyer and Westgate, 2004; Sreenivasulu et al., 2007). In some crops, selection for and use of stay-green types has been promoted as a means for combating drought stress susceptibility (Thomas and Howarth, 2000). However, the molecular basis of stay-green phenotype in barley (*Hordeum vulgare*) has not been explored in detail. As the flag leaf is the principal source organ, sustaining its photosynthetic activity under postanthesis drought stress is considered a strategy to mitigate the yield penalty. Water use efficiency (WUE) is the amount of biomass (carbon) accumulated per unit of water, hence an important trait under water-limited conditions (Condon and Richards, 1992; Rebetzke et al., 2002; Richards et al., 2002). Breeding for WUE is considered important for developing drought-tolerant crops (Blum, 1996; Richards, 1996; Richards et al., 2002). Genetic loci that control transpiration efficiency have been identified (Teulat et al., 2002; Hall et al., 2005; Juenger et al., 2005). In Arabidopsis (*Arabidopsis thaliana*), *ERECTA* as well as *HARDY* (encoding an APETALA2/Ethylene Responsive Factor-like transcription factor) genes influence transpiration efficiency (Masle et al., 2005; Karaba et al., 2007).

[1] This work was supported by the German Federal Ministry of Education and Research (project GABI–GRAIN: integrative genomics approach for exploring seed quality and yield under terminal drought; grant nos. FKZ 0315041A and FKZ 0315041C; and grant nos. ProNET–T3 and 03ISO2211B to L.E.-L. and J.L.), the Internationales Büro-German Federal Ministry of Education and Research (grant no. IND09/526), and the German Research Foundation program (grant no. SFB648 to L.E.-L. and J.L.).

[2] These authors contributed equally to the article.

[3] Present address: Grain Quality and Nutrition Center, International Rice Research Institute, Metro Manila 1301, Philippines.

* Address correspondence to srinivas@ipk-gatersleben.de.

The author responsible for distribution of materials integral to the findings presented in this article in accordance with the policy described in the Instructions for Authors (www.plantphysiol.org) is: Nese Sreenivasulu (srinivas@ipk-gatersleben.de).

[C] Some figures in this article are displayed in color online but in black and white in the print edition.

[W] The online version of this article contains Web-only data.

[OPEN] Articles can be viewed online without a subscription.

www.plantphysiol.org/cgi/doi/10.1104/pp.113.229062

Abscisic acid (ABA) synthesis is a universal response of plants to drought, and this triggers major reprogramming of the transcriptome, stomatal closure, and restraint on transpirational water loss (Christmann et al., 2007; Cutler et al., 2010; Raghavendra et al., 2010), but this adaptation for survival inevitably reduces photosynthesis, grain filling, and grain yield. There is very little information on how WUE and other physiological parameters are influenced in genotypes that differ in ABA homeostasis. There have been several studies on altering ABA levels by overexpression of ABA biosynthesis or catabolism genes using constitutive promoters. For example, transgenic overexpression of 9-cis-epoxycarotenoid dioxygenase (*NCED*) genes in tomato (*Solanum lycopersicum*), Arabidopsis, bean (*Phaseolus vulgaris*), and cowpea (*Vigna unguiculata*) enhances ABA content in leaves or whole plants and reduces transpiration (Thompson et al., 2000; Iuchi et al., 2001; Qin and Zeevaart, 2002; Aswath et al., 2005). However, ubiquitous expression causes growth retardation. Improved drought tolerance was observed when transgenic tobacco (*Nicotiana tabacum*) and Arabidopsis plants were subjected to stress by withholding irrigation (Iuchi et al., 2001; Qin and Zeevaart, 2002). However, the impact on yield was not reported. Overexpression of the genes for ABA catabolic enzymes Cytochrome P450 or ABA 8′-hydroxylase (ABA8′OH) decreased the ABA levels and caused an increase in the phaseic acid (PA) content (Millar et al., 2006; Umezawa et al., 2006; Yang and Zeevaart, 2006; Ji et al., 2011). When *ABA8′OH* was down-regulated in barley by an RNA interference (RNAi) approach, the ABA content increased (Gubler et al., 2008), but there is no information on the performance of these transgenics under stress conditions.

There is now a wealth of information on ABA signaling components. PYRABACTIN RESISTANCE1 (PYR1)/PYR1-LIKE (PYL)/REGULATORY COMPONENT OF ABA RECEPTOR (RCAR) proteins function as soluble ABA receptors (Ma et al., 2009; Park et al., 2009) and act in concert with type 2C protein phosphatase (PP2C)-Sucrose nonfermenting1-related protein kinase2 (SnRK2) complex (Umezawa et al., 2009, 2010; Vlad et al., 2009). Phosphorylated SnRK2 appears to be required for the activation of the ABA-induced transcriptional cascade. In the simplest model, binding of PYR/PYL/RCAR to ABA promotes interaction with PP2C, thereby inhibiting the phosphatase activity of PP2C; as a result, phosphorylated SnRK2s can activate the relevant transcription factors (Kline et al., 2010). An increase in endogenous ABA resulting from environmental and/or developmental cues would then lead to the sequestration of PP2C and resultant activation of SnRK2s and their downstream ABA-responsive element binding protein (AREB)/ABA-responsive element binding factor (ABF)/basic-leucine zipper (b-ZIP) proteins and anion channels (Cutler et al., 2010; Hubbard et al., 2010; Klingler et al., 2010; Umezawa et al., 2010). The complete pathway from perception by PYR/PYL/RCARs to the activation of AREB/ABFs has been validated by transient expression experiments in Arabidopsis mesophyll protoplasts (Fujii et al., 2009). PYR/PYL/RCAR protein family members have been identified in rice (*Oryza sativa*), maize (*Zea mays*), sorghum (*Sorghum bicolor*), soybean (*Glycine max*), grapevine (*Vitis vinifera*), citrus (*Citrus sinensis*), and tomato (Klingler et al., 2010; Sun et al., 2011; Boneh et al., 2012; Kim et al., 2012; Romero et al., 2012). However, there is only sparse information on transcriptional regulation of diverse members of ABA receptors, especially in response to different levels of ABA (McCourt and Creelman, 2008; Umezawa et al., 2010).

How different levels of ABA impact ABA perception via the family of receptors and affect WUE in crop plants remains to be systematically explored. In this study, we addressed ABA homeostasis and WUE in barley. We employed a pair of breeding lines having a contrasting phenotypic response to drought. One line senesces, while the other line shows a stay-green phenotype. Additionally, we investigated transgenic lines that we generated wherein ABA metabolism was altered by promoting biosynthesis or by diminishing catabolism under control of a drought-inducible promoter. These investigations afforded a hitherto unavailable account of ABA dosage-dependent responses in the ABA signalosome vis-à-vis WUE over short-term and long-term drought conditions. The information on a subset of ABA receptors will also be useful toward engineering cereal crops adapted to climate change.

RESULTS

Putative ABA Signaling-Related Genes in Barley

A set of putative ABA signaling genes in barley was defined on the basis of the sequence homology to Arabidopsis genes. Rice orthologs were included to provide a monocotyledonae reference. The Arabidopsis *PYR/PYL/RCAR* family has 14 members; of these, 13 act to inhibit the function of *PP2C* genes that act as negative regulators of ABA response. In barley, nine orthologs were identified (*HvPYR/PYL1* through *HvPYR/PYL9*), of which eight were present as full-length sequences (Table I). PYR/PYL/RCAR proteins have a major birch pollen allergen (Bet v 1) domain that provides a scaffold for binding hydrophobic ligands. All Bet v 1 proteins have been grouped within the large START domain superfamily (Iyer et al., 2001; Radauer et al., 2008). The residues required for ABA binding are located within domains that form two loops around the ABA molecule. The one having a consensus sequence SGLPA is referred to as the proline gate, and the other with the sequence GG(E/D)HRL is known as leucine latch (Melcher et al., 2009; Santiago et al., 2009a). Both structures are generally well conserved in the set of HvPYR/PYL proteins (Supplemental

Table I. *List of genes putatively involved in ABA signaling*

The table shows the following details: HarvEST unigene identification, full-length cDNA identification, Affymetrix identification, full length/partial, open reading frame size, predicted molecular mass for the deduced proteins, predicted subcellular localization, genomic sequence information, and derived 5′ upstream region of the translational start site.

Name	HarvEST_ID	fl cDNA_ID	Affymetrix_ID	Full/ Partial	ORF	Molecular Mass	Predicted Localization	Assembly1 Morex_ID	5′ Upstream Region
					bp	*kD*			*bp*
HvPYR/PYL1	35_6019	—	—	Full	618	22.2	Cytosol	contig_120100	1,212
								contig_1036022	—
HvPYR/PYL2	35_47387	—	—	Full	531	20.1	Cytosol	contig_1029272	560
HvPYR/PYL3	35_2538	AK361631	—	Full	675	23.4	Cytosol	contig_7680	783
								contig_125541	—
HvPYR/PYL4	35_2536; 35_2537	AK376521	contig7717_s_at	Full	846	30.1	Chloroplast	contig_520617	1,215
								contig_1022368	—
HvPYR/PYL5	35_4843; 35_4842	AK363238; AK360170	—	Full	639	22.6	Cytosol	contig_9218	—
								contig_17013	—
								contig_2712	—
HvPYR/PYL6	35_27243	—	contig26435_at	Full	600	21.7	Chloroplast	contig_2167379	1,210
HvPYR/PYL7	35_26005	—	—	3′ Partial	430		Chloroplast	contig_1050478	—
HvPYR/PYL8	35_39062	—	—	Full	591	21.2	Cytosol	contig_59536	295
HvPYR/PYL9		AK362590	—	Full	621	22	Chloroplast	contig_6622	2,643
HvPP2C1	35_20474	AK356066	contig13161_at	Full	1,152	40.7	Cytosol	contig_141492	1,381
HvPP2C2	35_16690	AK362128	contig9099_at	Full	1,155	41.1	Chloroplast	contig_4567	—
HvPP2C3	35_9808	AK358849	—	Full	780	27	Chloroplast/ cytosol	contig_121052	1,500
HvPP2C4	35_18890	AK251854	contig9585_at	Full	1,434	49.7	Chloroplast	contig_2186347	997
								contig_1024074	—
								contig_2652	—
HvPP2C5	35_8070	AK374059	contig18582_at	Full	1,197	42.2	Chloroplast	contig_120142	1,500
								contig_1015267	—
HvPP2C6	35_7671	AK377029	contig17128_at	Full	1,089	39.4	Nucleus	contig_145966	1,500
								contig_1023418	—
								contig_2168525	—
								contig_605940	—
HvPKABA1/ HvSnRK2.1	35_3036; 35_31805	AK372880	contig_1561710	Full	1,029	38.8	Cytosol	contig_48093	1,500
								contig_1010515	—
HvSnRK2.2	35_15989	AK250358	—	Full	1,074	40.9	Cytosol	contig_1016754	1500
								contig_49192	—
HvSnRK2.3	35_16858	—	—	Full	1,089	41.9	Cytosol	contig_2162606	—
HvSnRK2.4	35_2796	AK374298	contig_160473	Full	1,101	41.5	Cytosol	contig_59002	1,500
								contig_1010711	—
HvSnRK2.5	35_15228	AK363699	contig_160302	Full	1,086	40.6	Cytosol	contig_256359	1,099
HvSnRK2.6	35_15990	AK367758; AK355634	contig_127028	Full	1,074	40.1	Cytosol	contig_114539	703
HvSnRK2.7	35_21442	AK251684	—	Full	1,026	38.5	Cytosol	contig_41066	1,500
HvSnRK2.8	35_16493	AK374249; AK366400	contig_5609	Full	1,026	38.6	Cytosol	contig_102922	—
HvSnRK2.9	35_20178	AK362030	—	Full	1,182	44.2	Cytosol	contig_45417	1,500
HvABI5	35_37023; 35_22244	AK373571; AK371351	contig15335_s_at	Full	1,062	37.7	Nucleus	contig_99412	1,500

Fig. S1A), although within the Pro gate, an S residue is replaced by T in HvPYR/PYL1and an A by G in HvPYR/PYL9; within the HvPYR/PYL2 Leu latch, GGEHRL appears as DGNHPL. The phylogenetic analysis shown in Figure 1A suggested that HvPYR/PYL1 and HvPYR/PYL2 are both members of the same subfamily 1 as Arabidopsis AtPYL7 through AtPYL10, and HvPYR/PYL5, HvPYR/PYL6, and HvPYR/PYL8 are similar to Arabidopsis subfamily 3 (AtPYR1 and AtPYL1 through AtPYL3). HvPYR/PYL3, HvPYR/PYL4, HvPYR/PYL7, and HvPYR/PYL9 cluster with three rice proteins to form a separate clade. No HvPYR/PYL proteins could be assigned to Arabidopsis subfamily 2 comprising AtPYL4 through AtPYL6 and AtPYL11 through AtPYL13.

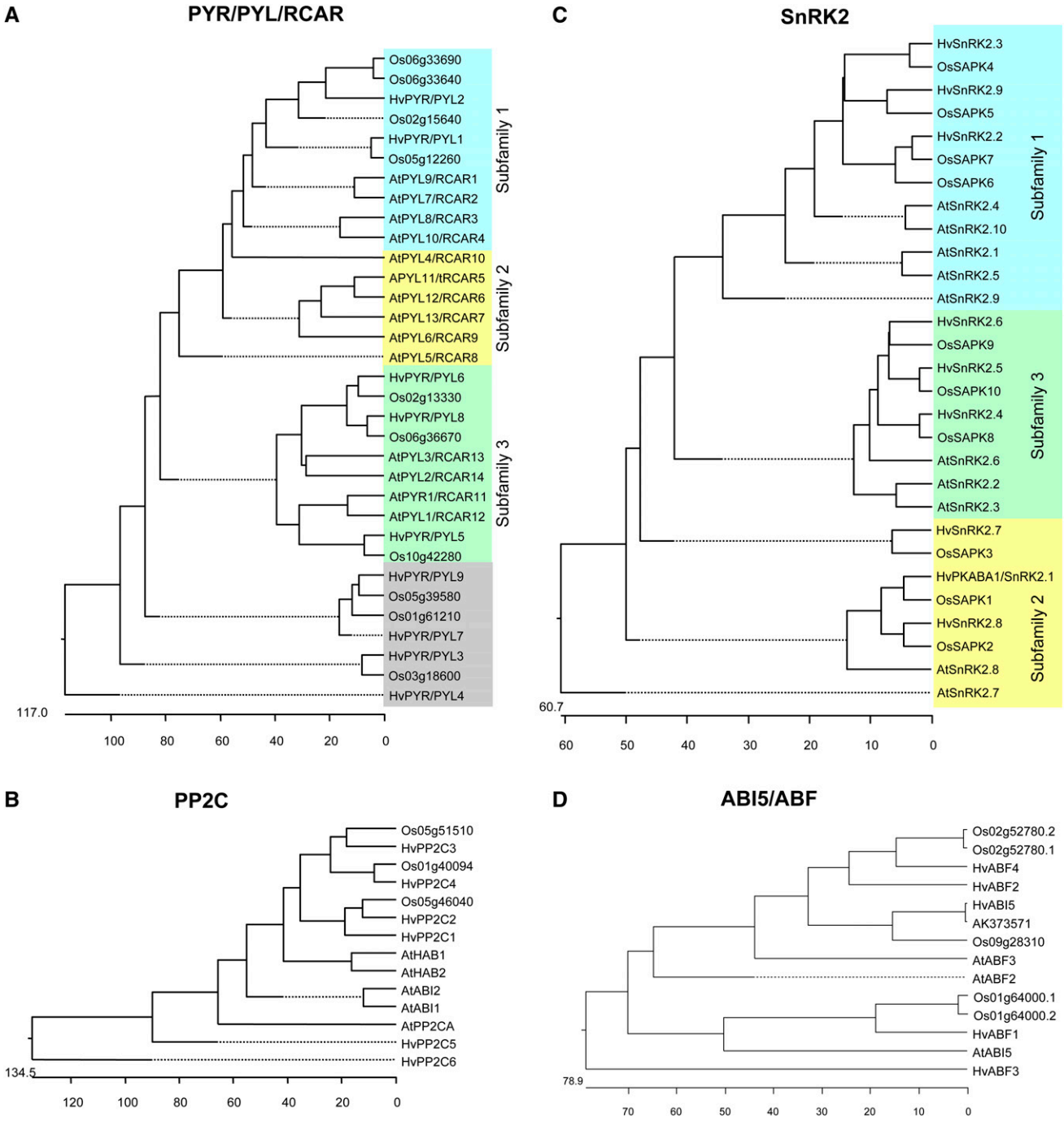

Figure 1. Phylogenetic trees of different families of ABA signaling. Protein alignments were done using ClustalW (MegAlign, DNAStar) with sequences from Arabidopsis, rice, and barley. Subfamilies are shaded in different colors. [See online article for color version of this figure.]

Six *PP2C* orthologs were identified (*HvPP2C1* through *HvPP2C6*; Fig. 1B). Eleven conserved motifs have been associated with PP2C proteins (Bork et al., 1996). All these motifs are present in the deduced barley proteins, with the exception of HvPP2C3 containing only motifs 1 to 5 and HvPP2C6 lacking motifs 1, 3, and 9. (Supplemental Fig. S1B). These two proteins also lack the conserved Trp (W) residue, which is inserted between the PYR/PYL/RCAR Pro gate and Leu latch regions (Supplemental Fig. S1B).

The Arabidopsis SnRK2 family consists of 10 genes (Boudsocq et al., 2004). Of these, *AtSnRK2.2*, *AtSnRK2.3*, and *AtSnRK2.6* (all belonging to subfamily III) are directly involved in ABA signal perception. The

barley orthologs comprised nine full-length sequences. One of these, designated as *HvPKABA1/SnRK2.1*, has been characterized previously (Yamauchi et al., 2002). We designated the additional ones as *HvSnRK2.2* through *HvSnRK2.9*. These formed three phylogenetic clusters (Fig. 1C), SnRK2.2, SnRK2.3, and SnRK2.9 (subfamily 1), SnRK2.4, SnRK2.5, and SnRK2.6 (subfamily 3), and PKABA1/SnRK2.1, SnRK2.7, and SnRK2.8 (subfamily 2). ABA-dependent activation of the kinase and its interaction with Abscisic acid-insensitive1 (ABI1) requires an Asp-rich domain (Domain II) in the C terminus (Belin et al., 2006; Yoshida et al., 2006). Domain II was found in the C-terminal region in PKABA1/SnRK2.1, SnRK2.4, SnRK2.5, SnRK2.6, and SnRK2.8 (Supplemental Fig. S1C).

Members of the ABI5/ABF subfamily of bZIP transcription factors mediate ABA-induced transcription by interacting with ABA response promoter elements. Barley ABI5, ABF1, ABF2, and ABF3 have already been described as members of the bZIP transcription factor family, and we identified one additional partial clone (named HvABF4; Fig. 1D). HvABI5 forms a subgroup with AtABF2 and AtABF3 in phylogenetic comparisons, while HvABF1 seems to be orthologous to AtABI5 (Fig. 1D).

The Stay-Green and Senescing Types of Barley Show Differential Photosynthetic Efficiency and WUE under Terminal Drought

Senescence is a normal and eventual response of plants experiencing terminal drought. Screening 16 elite barley breeding lines for terminal drought tolerance identified a line that showed stay-green Lochow-Petkus (LP103) phenotype. This stay-green line displayed a reasonable level of drought tolerance and produced a superior grain weight (Fig. 2; Supplemental Fig. S2). The other lines senesced and gave lower yields. Among them, LP110 was chosen as a representative of the senescing lines. Withholding water for 3 weeks induced senescence in the leaves and spikes of line LP110 (Fig. 2B). By contrast, LP103 plants remained green for longer duration before senescence ensued under postanthesis drought (Fig. 2A). Stomatal conductance, transpiration, and assimilation were markedly inhibited by drought in the senescing line, but assimilation was maintained at a higher level in the stay-green line than in the senescing line under stress (Fig. 2, E–H). The WUE in senescing plants but not in stay-green ones was reduced by 1 week of drought stress exposure (Fig. 2H). The maintenance of WUE allowed the drought-stressed stay-green plants to produce larger grains in contrast to the senescing ones (Fig. 2D). This result was reproducible over two cropping seasons. The thousand grain weight in the stay-green type, unlike in the senescing genotype, was not compromised in drought conditions (Fig. 2D).

Altered ABA Flux and Expression Dynamics of ABA Perception and Sensor Genes in Stay-Green and Senescing Lines

ABA accumulated to higher levels (15-fold) in the flag leaf of drought-stressed senescing line than in the stay-green line. The difference was most pronounced in the early part of the grain-filling period, when the plants had been exposed to 4 d of drought stress (Fig. 2J). By 12 d after stress (DAS), the ABA level in the flag leaf of the senescing line began to fall but still remained at a higher level than in the control plants that had been watered regularly. The behavior of the stay-green plants was different; throughout the period of stress (4 and 12 DAS), the flag leaf ABA content had increased only about 3-fold over the level in irrigated plants. This level remained steady throughout the stress period (Fig. 2J). Both the assimilation rate and WUE were sustained better in stay-green line at 4 and 8 DAS (Fig. 2, E and H). The flag leaf tissue in drought-stressed senescing plants at 8 DAS contained more ABA catabolites (dihydrophaseic acid [DPA], 2.7-fold) and an inactive form of ABA (ABA-Glc ester, 4.5-fold; Fig. 2I; Supplemental Table S2). The stay-green line did not show this effect. Thus, ABA metabolism in the senescing genotype was highly sensitive to drought stress, while it was relatively unperturbed in the stay-green type with well-balanced ABA homeostasis.

Transcription of genes associated with ABA synthesis, degradation, and deconjugation was quantified using quantitative real-time (qRT) PCR (Supplemental Fig. S3). In congruence with the increase in the ABA content, *HvNCED2* transcript abundance in the flag leaf of the senescing line was 6-fold higher in stressed plants than in irrigated control plants at 8 DAS. By 12 DAS, however, *NCED2* transcription had diminished, while *barley β-glucosidase8* (*HvBG8*) expression had up-regulated, suggesting that increased ABA flux might operate through deconjugation events (Fig. 2I; Supplemental Fig. S3). By contrast, ABA homeostasis in the stay-green line was maintained via the moderate induction of *HvNCED2* and *HvBG8*.

The transcription profiles of ABA receptor/signaling genes also showed contrasting regulation in stay-green and senescing plants. At 8 DAS, only *HvPYR/PYL5* and *HvPYR/PYL7* were up-regulated in drought-stressed flag leaf of the stay-green line. During this stage, *HvPYR/PYL3*, *HvPYR/PYL4*, *HvPYR/PYL5*, *HvPYR/PYL6*, and *HvPYR/PYL8* were all down-regulated in drought-stressed flag leaf of the senescing line (Fig. 2K; Supplemental Fig. S4). Recall that ABA catabolite levels in plants under these conditions were elevated in stressed senescing plants but not in stay-green plants (Fig. 2I). Notably, five of the six genes (*HvPYR/PYL3*, *HvPYR/PYL4*, *HvPYR/PYL5*, *HvPYR/PYL6*, and *HvPYR/PYL8*) that we monitored were up-regulated in drought-stressed flag leaf at 12 DAS in senescing line plants, while none of them showed this change in the stay-green type (Supplemental Fig. S4). This suggests that the two lines differ in their capacity

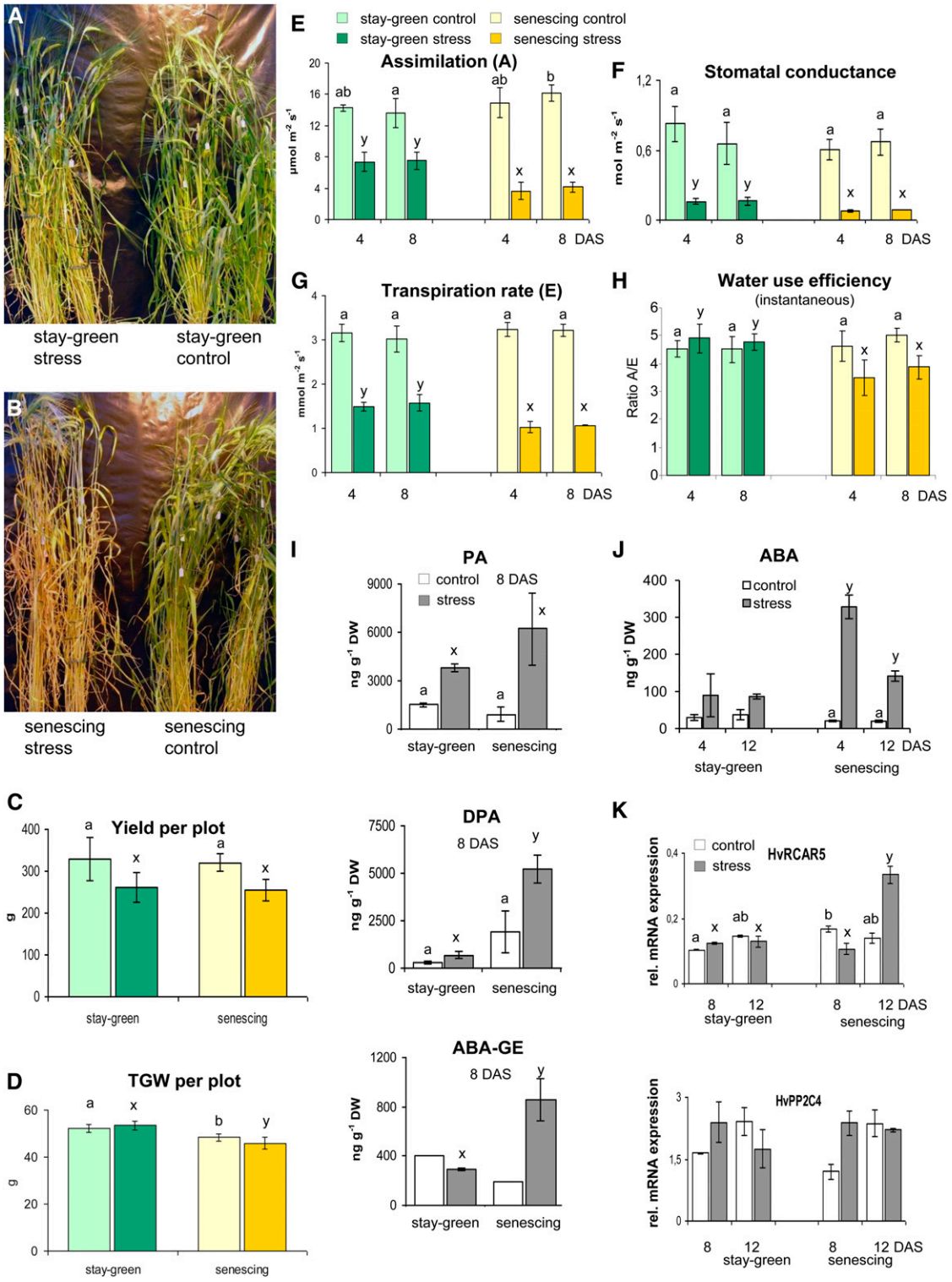

Figure 2. Phenotype of two contrasting barley genotypes under control and drought stress conditions. A and B, Plants of the stay-green (LP103) and senescing genotype (LP110) after 3 weeks of stress and respective control plants. C and D, Yield related parameters showing mean values ± SD with $n = 10$. E to H, Assimilation, stomatal conductance, transpiration rate, and instantaneous WUE (assimilation/transpiration) of the two genotypes measured in flag leaf at 4 and 8 DAS. The graphs show mean values ± SD with $n = 10$. I, ABA metabolites PA, DPA, and ABA-Glc ester measured in flag leaves 8 DAS. J, ABA levels in flag leaves after different stress duration in stay-green and senescing genotype. The graphs I and J show mean values ± SD with $n = 2$. K, Expression of *HvPYR/PYL5* and *HvPP2C4* in flag leaves at 8 and 12 DAS. The graphs show mean values from two replicates

to bind ABA and/or in their sensitivity to ABA. Despite the difference in the ABA levels in the flag leaf, most of the *PP2C* and *SnRK2* genes were markedly induced by stress in both stay-green and senescing plants (Supplemental Fig. S4).

Engineering ABA Biosynthesis and Catabolism Pathways to Alter ABA Flux under Postanthesis Drought

Two transgenic approaches were undertaken to alter ABA metabolism in barley, overexpression of *AtNCED6* that encodes the key enzyme for ABA biosynthesis and RNAi silencing to repress the endogenous *ABA8′OH* genes as a means to curtail ABA degradation. These transgene constructs were placed under control of the barley *late embryogenesis abundant* (*Lea*) B19.3 promoter, which is induced in vegetative tissues during postanthesis drought stress. Two independent homozygous transgenic lines of each construct were used for evaluation of the physiological performance under terminal drought stress. The lines will be referred to as LN for the *HvLea*::*AtNCED6* construct and LOHi for the *HvLea*::*Hv8′-hydroxylase* RNAi construct, respectively. In general, the transgenic plants performed better than the parental line (referred to as the wild type; WT) under stress. Both LN and LOHi lines possessed a higher relative leaf water content at 4 DAS (Fig. 3A). While the stress had a negative impact on assimilation in the wild type, the transgenic LN lines had higher assimilation rate, and LOHi lines suffered to a lesser extent (Fig. 3B). Instantaneous WUE (assimilation/transpiration) was not reduced in three of the four transgenic lines when they were subjected to drought stress. There was even an increase in LN transgenic lines (Fig. 3C). This contrasted the reduction seen in the wild type and one of the two LOHi lines. These results show effective coordination of assimilation with the balanced transpiration in LN plants under drought stress.

Expression of the transgene *AtNCED6* in flag leaves was detected as early as 0.5 DAS, and highest expression was observed at 8 DAS in both overexpression lines (LN39 and LN51), with nearly 2-fold increase under stress compared with control conditions (Fig. 4A). In the RNAi lines (LOHi236 and LOHi272), reduction in *HvABA8′OH1* transcript levels in flag leaves was observed mainly under long-term stress (12 DAS), with a clear reduction of 52% and 42% in LOHi236 and LOHi272 lines, respectively. Among three *HvABA8′OH* genes, only *HvABA8′OH-1* was induced under stress in the wild type (Fig. 4B, inset). Therefore, we focused on *HvABA8′OH-1*.

We measured the ABA content in the flag leaf of the wild type and transgenic lines under control and drought stress (0.5–12 DAS). This analysis showed that under the conditions of short-term drought stress at 2 DAS, much more ABA was accumulated in *AtNCED6* overexpression lines than in the wild type or in *ABA hydroxylase* RNAi lines (Fig. 4C). In the wild type, the highest level of ABA response was observed 2 d later than in LN39 (4 DAS, 17-fold), and these wild-type plants maintained higher ABA levels under long-term stress (12 DAS). By contrast, by 4 DAS onwards, LN39 plants had reduced their ABA levels and, under prolonged stress, maintained the ABA content at a near-basal level. This was also reflected in LN39 transgenic line, where down-regulation of endogenous *HvNCED1* gene is noted (Supplemental Fig. S5; Supplemental Table S3). In the LOHi line, ABA levels did not reach as high as in the wild type under long-term stress (4–12 DAS).

To understand the dynamics between ABA biosynthesis and degradation under short-term and long-term stress, we analyzed ABA catabolites in the wild type and in the ABA hydroxylase repression line (LOHi236) at 2 and 12 DAS. In the short term, the two major ABA degradation products PA and DPA increased similarly in the wild type and LOHi236 (2.8- and 1.8-fold for PA and 1.8- and 1.5-fold for DPA, respectively; Fig. 4D). While PA (9.2-fold) and DPA (6.4-fold) reached very high levels under long-term stress in wild-type plants (Fig. 4D), these degradation products accumulated to a lesser extent at 5.5- and 4.8-fold, respectively, in the LOHi236 RNAi plants.

Expression Dynamics of the ABA Receptor Complex Is Modulated Differentially in Transgenic Lines with Altered ABA Flux under Terminal Drought

Having determined that *AtNCED6*-overexpressing lines and *ABA8′OH RNAi* lines differ with respect to altered ABA flux and homeostasis under short-term versus long-term stress during the grain-filling period, we investigated regulation of *HvPYR/PYL* family

Figure 2. (*Continued.*)
of qRT-PCR-experiments from biological independent material ($n = 2$) with an additional two technical replications. Relative mRNA levels to reference gene HZ42K12 are shown by white and gray bars (mean ± SD). TGW, Thousand grain weight; ABA-GE, ABA Glc ester; DW, dry weight. Statistical analysis was carried out across genotypes for a given treatment using one-way ANOVA at $\alpha = 0.05$ with Tukey's posthoc test (E–H and K). Letters a and b and x and y represent statistical differences under control and stress conditions, respectively. Bars with similar or no letters indicate no statistical difference among genotypes under a given treatment. Two-way ANOVA performed to identify the signified difference between accessions (stay-green versus senescing lines) and condition (control versus drought stress) with *P* values of the *f*-test; $\alpha = 0.05$ and 0.01. For further details, see Supplemental Table S3.

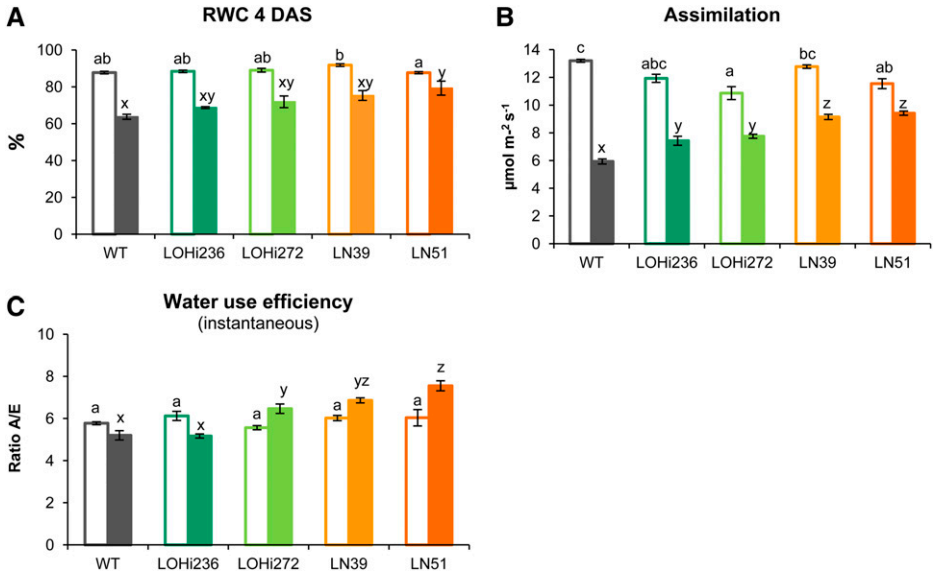

Figure 3. Physiological performance of the transgenic lines LOHi and LN compared with the wild type (WT) under control and drought stress conditions. A, Relative leaf water content (RWC) estimated at 4 DAS. B and C, Assimilation rate and calculated instantaneous WUE (assimilation [A]/transpiration [E]) in the wild type and transgenic plants. Mean values ± SE are given with $n = 15$ for all the parameters. White and filled bars represent control and stress conditions, respectively. Statistical significant differences among genotypes and a given treatment have been calculated using one-way ANOVA at $\alpha = 0.01$ with Tukey's posthoc test. Letters a, b, and c and x, y, and z represent statistical differences under control and stress conditions, respectively. Additional information of two-way ANOVA is provided in Supplemental Table S4.

members (Fig. 5). In general, *HvPYR/PYL* members (exception of *HvPYR/PYL1 and HvPYR/PYL5)* were down-regulated in the wild type and in both transgenic lines under stress (Fig. 5). Under short-term stress (2 DAS), *HvPYR/PYL5* was up-regulated in the flag leaf of line LN39; this coincided with ABA accumulation reaching its peak level. The transcript levels did not change in the RNAi line. In the wild type, up-regulation of *HvPYR/PYL5* was found at 4 DAS, when the ABA level had peaked (Fig. 5). Under prolonged drought stress (12 DAS), there were no stress-associated differences in the expression of *HvPYR/PYL1* and *HvPYR/PYL5* in any of these lines, but transgenic lines showed highest repression in LN39 and LOHi236 transgenic lines under long-term stress (Fig. 5; Supplemental Table S3). These results suggest that the wild type and transgenic line LN39/LOHi236 likely differ in their source tissues with respect to ABA binding and/or ABA sensitivity under short-term drought stress.

In general, transcriptional up-regulation under stress was observed for the PP2Cs (Supplemental Fig. S6). Notably, the up-regulation of *PP2C* genes in LN39 and LOHi236 was mainly confined to short-term drought stress, and in particular, the induction of PP2C1, 4 and 5 transcript accumulation was moderate in LOHi236 during 12 DAS. The *SnRK2*-related protein kinase genes (*HvPKABA1/SnRK2.1* and *HvSnRK2.7*) were up-regulated under short-term drought stress in LN39. The relative expression levels of *HvPKABA1/SnRK2.1* and *HvSnRK2.7* in LOHi236 line were lower during midterm stress compared with the wild type and LN39. Notably, this line produced less ABA under stress compared with the wild type.

Three-Dimensional Modeling of HvPYR/PYL Protein Structures

As outlined in "Materials and Methods," we constructed three-dimensional models for three HvPYR/PYL proteins in I-TASSER (Roy et al., 2010). We selected HvPYR/PYL5 (that shows highest homology to Arabidopsis AtPYR1/RCAR11) as well as HvPYR/PYL1 and HvPYR/PYL2 that show some differences in the amino acid sequence of the gate and latch regions, respectively (Fig. 6A). The general structure of the predicted models (best scores) has an α-β-α2-β6-α topology (Fig. 6A) and exhibits very similar helix-grip folds compared with AtPYR1 and AtPYL2, a characteristic of the START protein superfamily (Iyer et al., 2001). Interestingly, HvPYR/PYL5 has an additional α-helix in the N-terminal region (residues 5–12) but lacks the small helical segment 3 that is usually followed by six β-strands (Fig. 6B). The largest α-helix consisting of 30 amino acids is located at the C-terminal part of the protein. HvPYR/PYL1, unlike HvPYR/PYL5, does not haves β-strands 2 and 3; in HvPYR/PYL2, these two β-strands are predicted as a very short segment of only three amino acid residues (Fig. 6, A, C, and D). Additionally, like *HvPYR/PYL5*, *HvPYR/PYL1* does not contain

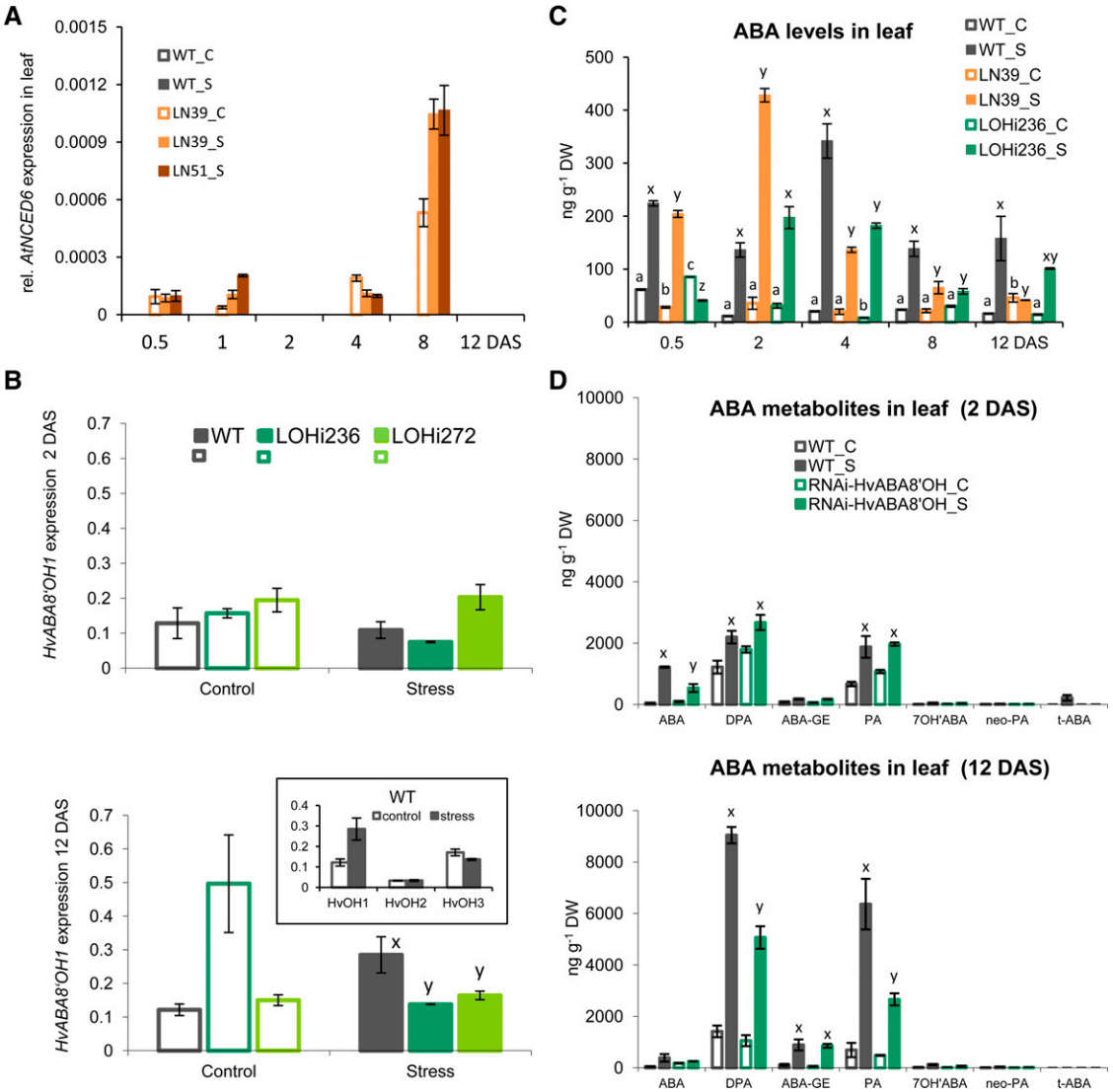

Figure 4. Expression levels of *AtNCED6* and *HvABA8′OH1*, ABA, and ABA metabolite levels in the wild type (WT) and transgenic lines under control and drought stress conditions. A, *AtNCED6* expression in leaf tissue of two transgenic *LeaNCED6* lines (LN) at different time points after stress induction analyzed by qRT-PCR. B, Expression of *HvABA8′OH1* in two RNAi lines *LeaABA8′OH* (LOHi). Relative expression to reference gene HZ42K12 in leaf tissue at 2 (top graph) and 12 DAS (bottom graph) is shown. The small graph within the bottom diagram represents the expression of three ABA hydroxylase genes in the barley wild type. C, ABA levels in the wild type, LN, and LOHi plants. D, Levels of ABA metabolites under short- and long-term stress in the wild type and RNAi line. White and filled bars represent control and drought stress, respectively. C, Control; S, stress; ABA, cis-ABA; ABA-GE, ABA Glc ester; 7′OH-ABA, 7′-Hydroxy-ABA; t-ABA, trans-ABA; DW, dry weight. Statistically significant differences among genotypes and a given treatment have been calculated using one-way ANOVA at $\alpha = 0.05$ (C and D) with Tukey's posthoc test. Letters a, b, and c and x, y, and z represent statistical differences under control and stress conditions, respectively. Two-way ANOVA tests have been calculated to show differences between control and stress with $*P \leq 0.05$ and $**P \leq 0.001$ to calculate statistically significant differences. Additional information of two-way ANOVA is provided in Supplemental Table S4.

α-helix 3. The sequence and structure of the gate loop (between β-strands 3 and 4) and the latch region (between β-strands 5 and 6) of HvPYR/PYL5 are identical to those present in Arabidopsis PYR/PYL/RCARs (Fig. 6B, middle). By contrast, the gate and latch regions differ slightly in HvPYR/PYL1 (Fig. 6C, middle; Supplemental Fig. S1A), and the latch region differs in HvPYR/PYL2 (Fig. 6D, middle; Supplemental Fig. S1A). Although the primary structure does differ slightly, the three-dimensional modeling indicates that the gate and latch regions can have loop-like structures. Figure 2, B to D, indicates putative ligand binding sites in the gate and latch regions. It will be interesting to determine if

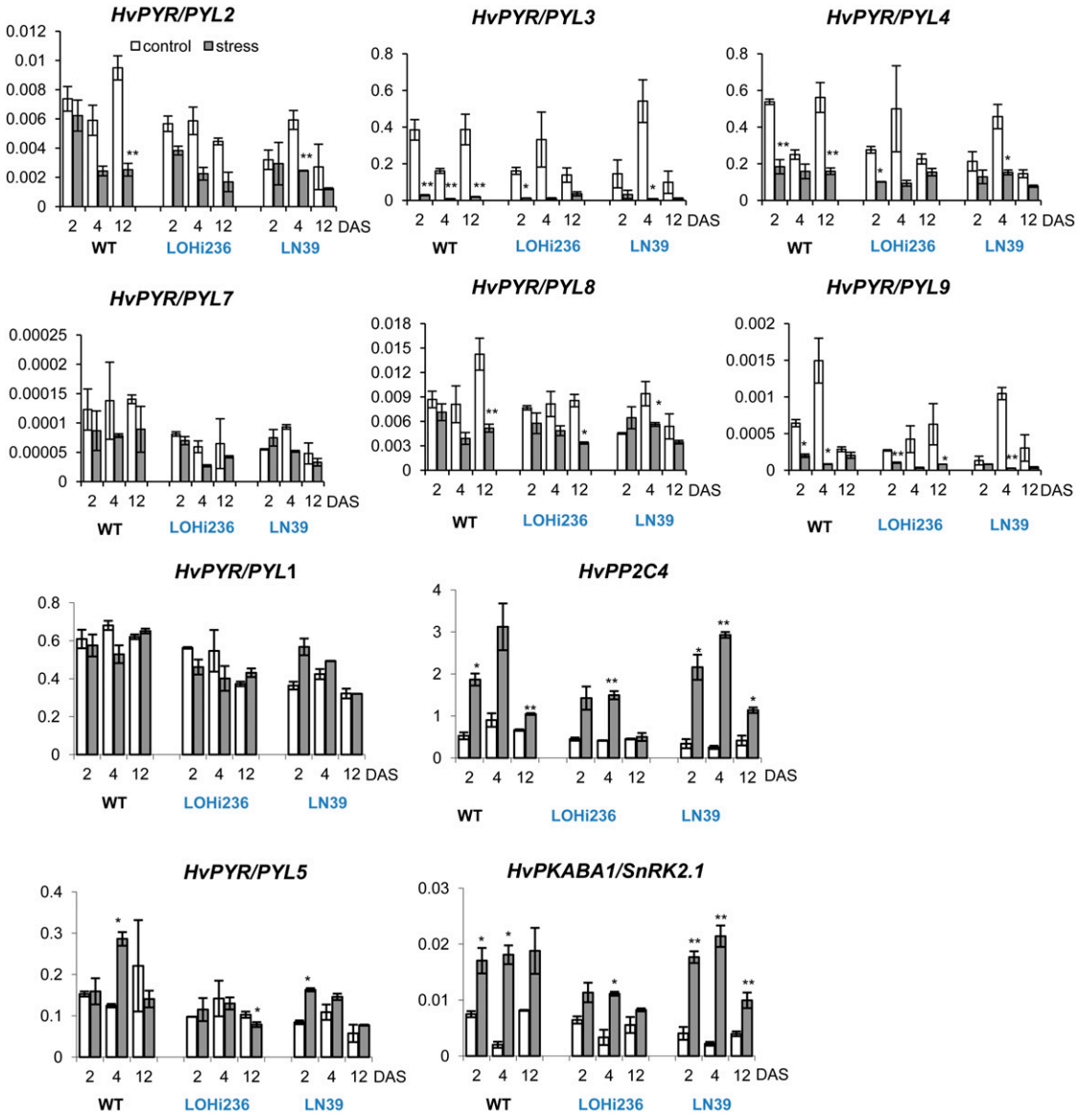

Figure 5. Differential expression of putative ABA signaling genes in barley wild type (WT) and transgenic plants under terminal drought stress analyzed by qRT-PCR. Differentially expressed genes in flag leaves that experienced different duration of stress (2, 4, and 12 DAS). LOHi236 indicates RNAi line *LeaABA8′OH*, and LN39 indicates *LeaNCED6* overexpression. The graphs show mean values from two replicates of qRT-PCR experiments from biological independent material ($n = 2$) with an additional two technical replications. Relative mRNA levels to reference gene HZ42K12 are shown by white and gray bars (mean ± SD). The significance of differences between control and stress was determined using two-way ANOVA, with $*P \leq 0.05$ and $**P \leq 0.001$. Statistically significant differences across genotypes were calculated using one-way ANOVA and are given in Supplemental Table S4. [See online article for color version of this figure.]

the predicted structural differences influence functional properties.

Physical Interaction of the ABA Receptor Components

A yeast (*Saccharomyces cerevisiae*) two-hybrid (Y2H) assay was conducted to examine interactions between selected HvPYR/PYLs and HvPP2C4. HvPYR/PYL1, HvPYR/PYL2, and HvPYR/PYL5 were fused to the GAL4 DNA binding domain and HvPP2C4 was fused to the GAL4 activation domain to circumvent self-activation of the Y2H gene reporters. After cotransforming the cloned genes in pairs into the yeast strain MaV203, interaction between receptor and phosphatase was tested on medium with (100 μM ABA) or without ABA supplementation. In this study, HvPYR/PYL1 interacted with HvPP2C4 in the presence of ABA, while a weaker interaction was noted in the absence of ABA. HvPYR/PYL5-HvPP2C4 interaction was ABA dependent (Fig. 7). By contrast, no

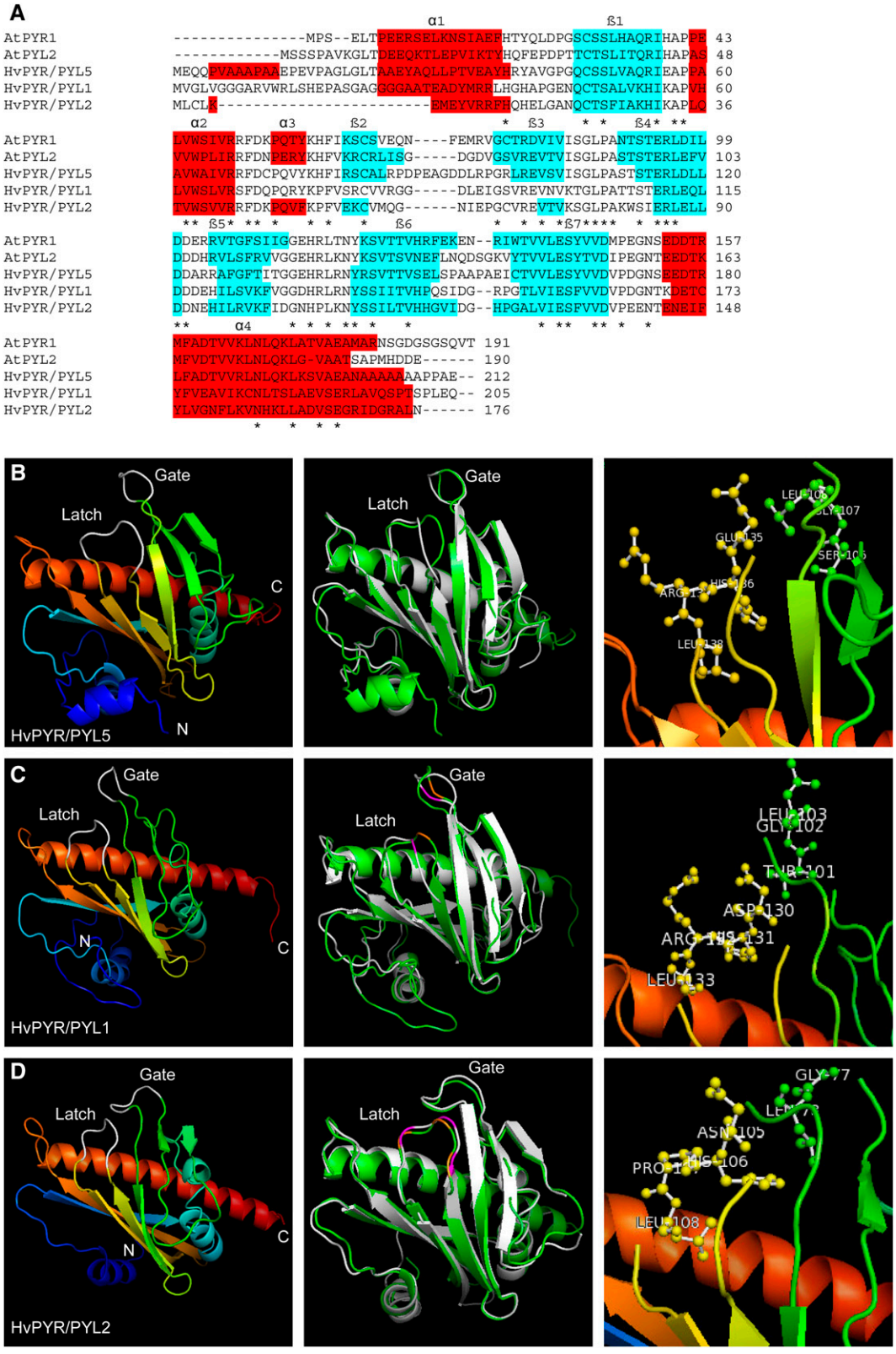

Figure 6. Structural similarities between HvPYR/PYL5, HvPYR/PYL1, and HvPYR/PYL2 and two members of the Arabidopsis RCAR/PYR/PYL family. Three-dimensional models have been generated using I-TASSER and further processed with PyMOL software. A, Amino acid sequence alignment. Identical residues are indicated by asterisks, and predicted α-helical and β-sheet structures are highlighted in red and blue, respectively. Remaining residues are coils. B, C, and D, Predicted three-dimensional

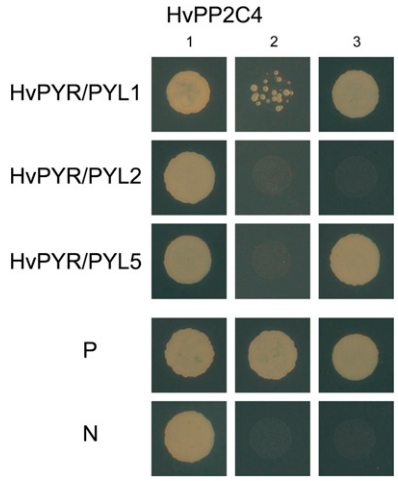

Figure 7. Interaction of HvPYR/PYL1 and HvPYR/PYL5 with HvPP2C4 in a Y2H assay using the HIS reporter. HvPYR/PYLs-binding domain fusions were coexpressed with HvPP2C4-activation domain and tested for positive interactions without (2) or with ABA (3) or cotransformation (control, 1). Positive (P) and negative (N) controls were provided by the Invitrogen Y2H Kit. The numbers above the columns indicate the medium as follow: SC-Leu-Trp (1), SC-Leu-Trp-His plus 50 mm 3-AT (2), and SC-Leu-Trp-His plus 50 mm 3-AT and 100 μM ABA (3). [See online article for color version of this figure.]

interaction was found between HvPYR/PYL2 and HvPP2C4 regardless of ABA addition. Note the amino acid changes in HvPYR/PYL2 in the core latch region that is necessary for ABA binding (Supplemental Fig. S1A). This region seems to be important for interaction with PP2C. In summary, all three tested HvPYR/PYL proteins behaved differently in the Y2H screening.

To validate the interactions in planta, bimolecular fluorescence complementation (BiFC) analysis was employed (Fig. 8). Fluorescence was detected predominantly in the cytoplasm and nucleus for the combinations of dimer formation of HvPYR/PYL5, HvPP2C4-HvPYR/PYL5, and HvPP2C4-HvPKABA1/SnRK2.1 complexes. This finding is in agreement with the interaction of Arabidopsis ABI1-AtPYL9, which takes place in the nucleus and cytosol (Ma et al., 2009). However, in rice, it was shown recently that the complex of OsPYL/RCAR5-OsPP2C30 formed exclusively in the nucleus (Kim et al., 2012). Adding ABA to the protoplasts caused no changes in the interaction. Imposing desiccation stress with polyethyleneglycol or mannitol treatment of protoplasts also did not change the interactions (Supplemental Fig. S7). The interaction of HvPYR/PYL5 with HvPP2C4 noted using BiFC (Fig. 8) fits with Y2H data. However, in contrast to the Y2H results, no interaction between HvPYR/PYL1 and HvPP2C4 was detected (data not shown). Additionally, we could demonstrate interaction between HvPP2C4 and HvPKABA1/SnRK2.1 by BiFC (Fig. 8). This combination could not be tested in Y2H due to self-activation problems with both proteins (data not shown). In summary, a complete ABA signaling complex consisting of barley HvPYR/PYL5, PP2C4, and PKABA1/SnRK2.1 is formed in planta, suggesting a highly conserved mechanism in monocots and dicots.

DISCUSSION

Selection for higher WUE using quantitative trait loci analysis has been undertaken as an approach to improve drought tolerance (Chen et al., 2011; Zhengbin et al., 2011). However, the genes for the trait have not yet been isolated in cereals. From a physiological perspective, it is well known that ABA accumulation in response to drought reduces transpirational water loss and helps plants survive, but under long-term stress, it is at the expense of photosynthetic productivity (Yoo et al., 2010). Hence, understanding the fine regulation of stomatal functions by ABA under short-term versus long-term stress is important for devising strategies to improve WUE and drought tolerance in crops (Sreenivasulu et al., 2012). There is clear evidence from studies on isolated leaf epidermis or guard cell protoplasts for the participatory role of ABA signaling complex in affording ABA sensitivity and reduction of water loss. However, the impact of any differences in the ABA content and that of the activity of the ABA signaling components on plant growth and development under conditions of prolonged stress are unclear (Ben-Ari, 2012; Merilo et al., 2013). In our study, we have addressed this by investigating a pair of elite breeding lines of barley, a line that senesces sooner under drought (senescing line; LP110) and a line that remains green for a longer duration (stay green; LP103) despite the stress. In addition, we have used, in this study, transgenic barley lines that have been engineered for drought-inducible ABA production or diminution of ABA catabolism to alter ABA homeostasis.

Importance of ABA Homeostasis in Improving WUE under Long-Term Drought Stress

The stay-green and senescing lines differed not only in their assimilation performance under stress, but also

Figure 6. (*Continued.*)
models (best score) of HvPYR/PYL5 (B), HvPYR/PYL1 (C), and HvPYR/PYL2 (D). At left, N and C termini are indicated, and gate and latch regions are shown in white. The middle shows an overlay with the top hit structural Arabidopsis analog (AtPYL2 for HvPYR/PYL5 and HvPYR/PYL1, AtPYR1 for HvPYR/PYL2) generated with PyMOL. Green indicates the HvPYR/PYL sequence, white indicates the Arabidopsis RCAR/PYR/PYL sequence, and orange- and magenta-labeled residues indicate different amino acids at that position. At right, predicted ligand binding sites within the gate and latch regions and amino acid residues and their position within the protein sequence are indicated.

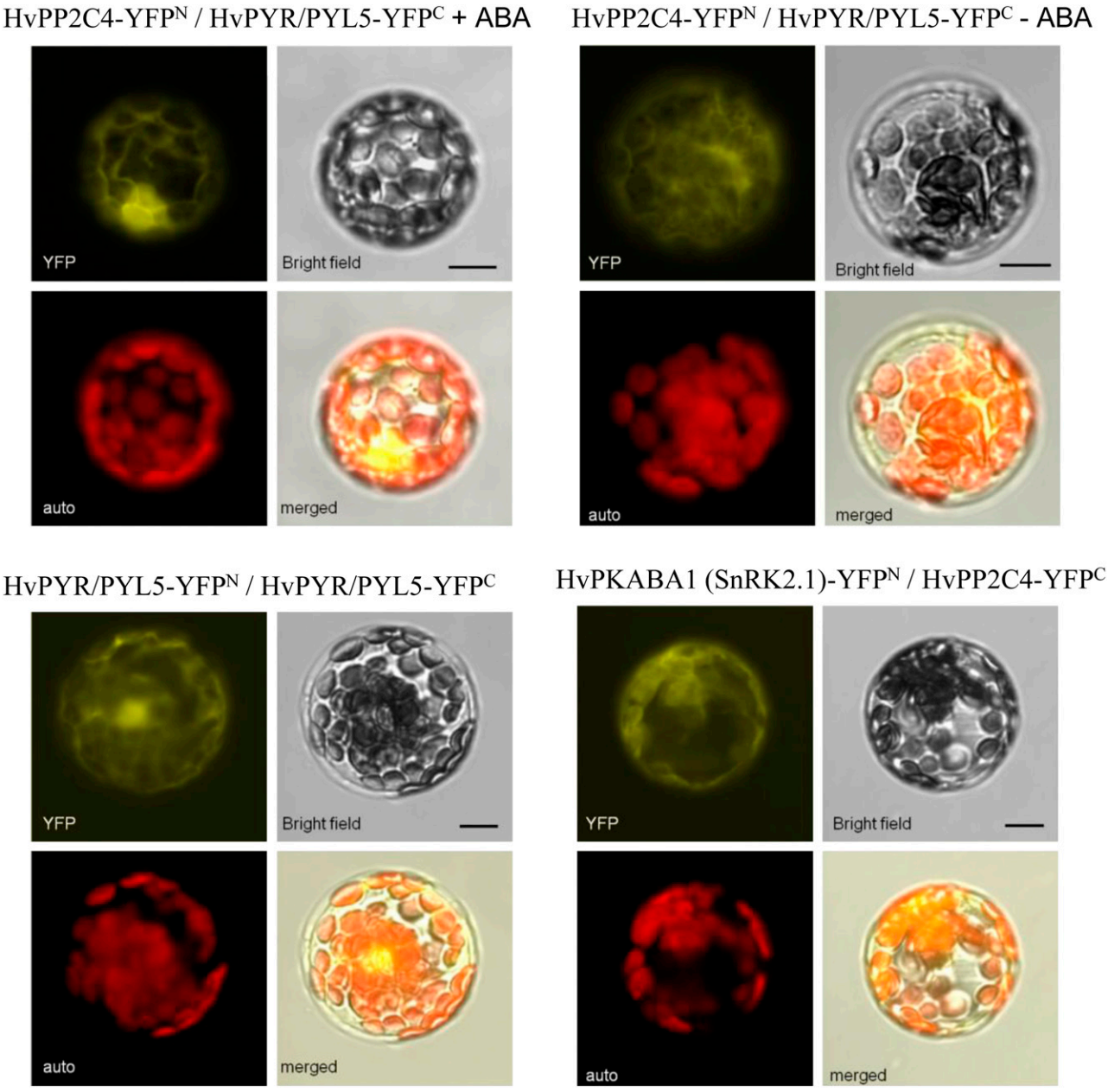

Figure 8. Interaction of ABA receptor components analyzed by BiFC. Pairs of PYR/PYL5-YFP^C/PP2C4-YFP^N, PYR/PYL5-YFP^C/PYR/PYL5-YFP^N, and PP2C4-YFP^C/PKABA1/SNRK2.1-YFP^N were transformed into Arabidopsis protoplasts. Fluorescence images were taken 1 d after transformation. The pictures are YFP, bright field, autofluorescence (auto), and merged images.

in ABA metabolism. The senescing line synthesized far greater levels of ABA than the stay-green line under short-term stress, and it continued to maintain a high level of ABA and ABA catabolites under long-term stress. Consistent with the observations that ABA catabolism is triggered to degrade excess ABA (Cutler and Krochko, 1999), we found that ABA and also ABA catabolites accumulated in a senescing breeding line of barley under drought stress (Seiler et al., 2011). This indicates a greater flux in ABA metabolism, affecting WUE and assimilation negatively in the senescing line. By contrast, the relatively modest increase of ABA in the stay-green line was held in check over long-term stress, and this homeostasis appeared to help the line sustain WUE and assimilation. Overaccumulation of ABA or constitutive activation of ABA signaling reduces WUE and thus growth (Sreenivasulu et al., 2012; Pizzio et al., 2013; Zhao et al., 2013). For example, overexpression of *NCED* under the control of *ribulose-1,5-bisphosphate carboxylase/oxygenase small subunit gene promoter*, which is highly active in photosynthetic tissues, causes leaf yellowing, reduced chlorophyll

content, and reduced growth rate (Gittins et al., 2000; Tung et al., 2008). The elevated ABA flux in our senescing line might have resulted in low xanthophyll content. These results emphasize that engineering WUE enhancement in barley entails more subtle changes to ABA metabolism that requires, as a prerequisite, delineation of the ABA signalosome components.

Because we found ABA homeostasis to influence instantaneous WUE distinctly in elite breeding lines, we manipulated endogenous ABA levels in transgenic barley under the control of a drought-inducible promoter. The rise in ABA accumulation under short-term stress in LN39 carrying chimeric *AtNCED* correlated with the expression of the transgene and also with remodulated expression of *HvNCED1* and *HvNCED2* genes (Fig. 4; Supplemental Fig. S5). While these plants responded by increasing their ABA content in the short term, they reprogrammed ABA metabolism to maintain a near-basal level over the long-term stress through apparent feedback control via down-regulation of *HvNCED* genes. These events appear to have held in check the ABA levels under long-term stress. This type of control over ABA homeostasis was lacking in the wild type, where *HvNCED2* expression seemed to contribute to the increase in ABA from 4 to 8 DAS and *HvNCED1* expression during 8 and 12 DAS (Supplemental Fig. S5). Thus, in the wild type, higher ABA levels remained throughout the stress period (Fig. 4C).

The net accumulation of ABA in LOHi236 (RNAi construct of *ABA8′OH*) was not as high as in *AtNCED* transgenic line at the early stages (2 DAS). In the wild type, long-term stress caused an increase in ABA flux, but, in LOHi236, where ABA catabolism has been repressed to some extent, the stress condition had a modest positive effect on net ABA production (Fig. 4D). Taken together with the observations that drought-induced *AtNCED6* expression was associated with down-regulation of *HvABA8′OH* genes and that this resulted in improved assimilation and WUE under terminal drought, the results reinforce the notion that plants under long-term stress benefit from modulated ABA homeostasis. These results support the inference that net rate of ABA accumulation in the wild type is highly and upwardly responsive to drought, while the dynamics of it is controlled tightly in the transgenic lines enhancing WUE.

Expression Dynamics of ABA Perception Genes under Short-Term versus Long-Term Drought Stress in Lines That Show Differences in ABA Flux

Given that many potential members of the ABA signalosome were identified in barley, it was of interest to elucidate their functional aspects. The highest ABA content (342 ng g^{-1} dry weight) seen in wild-type barley flag leaf was at 4 DAS, a time point at which higher expression of *PYR/PYL5* in flag leaf was witnessed. However, as a consequence of transgenic expression of *AtNCED*, the ABA levels reached 428 ng g^{-1} dry weight already at 2DAS, and under these conditions, *PYR/PYL1* and *PYR/PYL5* were also induced (Fig. 5). This suggests that differences in ABA levels can modulate the ABA signalosome by altering the expression of specific receptors in the family. In the RNAi line, where there was a moderate increase in ABA content that was less compared with the wild type, there were no changes in the transcript level. In Arabidopsis, it has been reported that an increase in ABA via either exogenous supply or enhanced production under water deficit conditions down-regulates *AtPYL8*, *AtPYL4*, *AtPYR1*, and *AtPYL1* expression; the other members remain constant or show slight up-regulation (Santiago et al., 2009b; Szostkiewicz et al., 2010). We found, in wild-type barley, no change in the expression of six *HvPYR/PYL* genes under short-term stress but down-regulation under prolonged stress (Fig. 5). In the senescing type of barley breeding line, elevated flag leaf ABA content down-regulated the transcription of ABA receptors when the plants reached midpoint in drought stress, but *HvPYR/PYL* transcription was again up-regulated when the ABA level had been reduced in long-term stress (Supplemental Fig. S4). No such adjustments in receptor gene expression were found in the stay-green type that maintained ABA homeostasis under long-term stress. Collectively, all these results point to different levels of ABA in short-term versus long-term stress having an impact on perception by various PYR/PYL members that appear to have specialized functions with respect to signaling dynamic cellular ABA content (Miyakawa et al., 2013; Okamoto et al., 2013).

Most barley *PP2C* and *SnRK2* members were prominently up-regulated under stress in the senescing and stay-green types, the wild type, and the LN39 transgenic line (Supplemental Figs. S4 and S6), regardless of the differences in the ABA content. A similar situation has been reported in Arabidopsis, where *PP2C* genes are elevated, while the majority of *PYR/PYL* members are down-regulated upon exogenous ABA treatment (Santiago et al., 2009b; Szostkiewicz et al., 2010). These authors also reported that ABA-related stress conditions or treatments alter the ratio of PP2C to PYR/PYL at both transcript and protein levels. Recently, it was postulated that an increase in this ratio might be necessary for activation of the downstream ABA signaling cascade under stress conditions (Chan, 2012). It is interesting to note that *PP2C*:*PYR/PYL* transcript ratio in the wild type was preferentially higher under stress, and this correlated with reduced WUE. The RNAi line that had a lower ABA flux than the wild type under stress showed an unaltered *PP2C*:*PYR/PYL* ratio; a similar situation was also found in the stay-green line that had a reduced ABA flux.

Receptor Combinations and ABA Responses under Postanthesis Drought Stress

PYR/PYL, PP2C, and SnRK2 families comprise many members, and various combinations of them in receptor complexes are conceivable. Structural differences in the members do impact WUE and drought tolerance. In Arabidopsis, overexpression of $PYL4^{A194T}$ mutant affords stress tolerance (Pizzio et al., 2013); overexpression of *AtPYL13*, which is known to differ from other PYLs in its ABA binding pocket, leads to improved drought tolerance (Zhao et al., 2013). Thus, some of the fine differences and expression levels in the signalosome components can have physiological consequences.

As shown in this study on barley and in other studies on Arabidopsis (Szostkiewicz et al., 2010; Pizzio et al., 2013; Zhao et al., 2013), the compositions of the receptor complexes affect sensitivity to and selectivity for ABA and impact WUE. The transcriptional activation of a subset of receptors (*HvPYR/PYL1* and *HvPYR/PYL5*) by elevated ABA under short-term stress in LN39 suggests that this complex is pertinent to mediate ABA signaling under these conditions. HvPYR/PYL5 belongs to subfamily 3 that includes the well-characterized AtPYR1 and AtPYL1. These form dimers in Arabidopsis (Miyazono et al., 2009; Santiago et al., 2009b; Yin et al., 2009; Dupeux et al., 2011). Our Y2H and yellow fluorescent protein (YFP) complementation experiments suggest that HvPYR/PYL5 forms a homodimer (Fig. 8). The three-dimensional model for HvPYR/PYL5 protein presented in Figure 6 includes the ABA-binding residues located within the domains that form two loops around the ABA molecule (Melcher et al., 2009; Santiago et al., 2009a). It is known that the Ser residue of the Pro gate (SGLPA) directly interacts with a catalytic Glu residue of AtABI1 (Miyazono et al., 2009). Thr is present instead of Ser in HvPYR/PYL1, and it did not dimerize in our analyses. Dimerization might prevent basal activation of the signaling pathway in the absence of ABA, as the interfaces of the receptors for homodimerization and PP2C binding are largely overlapping (Dupeux et al., 2011). After binding of ABA, the dimeric proteins dissociate to form the signaling complex. While monomeric receptors have a competitive advantage for binding to ABA and PP2Cs, monomeric and dimeric receptors can form high-affinity complexes with PP2C (Ma et al., 2009; Santiago et al., 2009b).

The monomeric proteins of Arabidopsis, AtPYL5, PYL6, and PYL8, show partial interaction with PP2C in absence of ABA. The dimeric receptors such as PYR1 and PYL1 do not interact under these conditions in Arabidopsis. Our findings in barley suggest a similar scenario as in Arabidopsis; barley PYR/PYL5, known to participate in homodimer formation, interacted with HvPP2C4 only in presence of ABA. By contrast, HvPYR/PYL1 showed weak interaction even in absence of ABA, hinting that the in planta oligomeric state of these two putative receptors is different. AtPYR1 residue H60 plays a key role in determining the oligomeric state of ABA receptors, and a H60P substitution leads to destabilization of the PYR1 dimer (Dupeux et al., 2011). HvPYR/PYL1 and HvPYR/PYL2 both contain a P residue at the corresponding position (H77 in HvPYR/PYL1 and H53 in HvPYR/PYL2), and this would explain the ABA-independent interaction of PYR/PYL1 with PP2C4 in the Y2H assays. The C terminus of HvPKABA1/SnRK2 includes an Asp-rich domain (Domain II) that is known to be required for both ABA-dependent activation of the kinase (Belin et al., 2006) and its interaction with ABI1 (Yoshida et al., 2006), and we found interaction between HvPP2C4 and HvPKABA1/SnRK2.1.

The overall implication is that plants employ PYR/PYL-ABA-PPC2 to fine-tune specific ABA signaling pathways in response to the prevailing levels of ABA (Santiago et al., 2012). The three major findings from our study supports general occurrence of this scenario. (1) The *PYR/PYL*, *PP2C*, and *SnRK2* gene family members are generally conserved across the monocot/dicot divide while exhibiting variation at the binding sites in selected members. (2) A drought-sensitive line of barley (senescing type) and the stay-green type differ remarkably in their regulation of *PYR/PYL* genes and also in their ABA levels over the course of postanthesis drought stress. The drought-sensitive plants that had high concentrations of ABA senesced, while the stay-green type plants modulated their *PYR/PYL* expression in the face of lower steady-state levels of ABA and survived longer under terminal drought. (3) Transgenic lines in which the ABA flux was modulated by expression of *NCED* (or an RNAi construct of *ABA8′OH*) under the control of a drought-inducible promoter corroborated the connectivity between ABA homeostasis, WUE, and PYR/PYL5:PP2C4 complex. Taken together, the results offer interesting insights into the combinations of active receptor complexes during postanthesis drought in barley and raise the prospects for improving WUE through conventional breeding of appropriate lines or through targeted transgenic approaches for fine manipulations of ABA flux and perception.

MATERIAL AND METHODS

Barley Gene Annotation of ABA Signaling Pathway

Barley (*Hordeum vulgare*) genes encoding proteins involved in ABA signaling were identified by a Blastn, Blastx, and tBlastx homology search of the 50,000 unigenes represented in the HarvEST database (http://harvest.ucr.edu), with the known Arabidopsis (*Arabidopsis thaliana*) and rice (*Oryza sativa*) ABA signaling sequences retrieved from the PubMed and TIGR databases, respectively (http://www.ncbi.nlm.nih.gov; http://rice.plantbiology.msu.edu/). The five best hits of each Blast search were selected and used to identify corresponding full complementary DNA (cDNA) sequences, using 24K full-length barley cDNA database (Matsumoto et al., 2011). The in silico translation product of each cDNA was queried for the presence of conserved domains identified in Arabidopsis. Multiple sequence alignments were performed using ClustalW (DNAStar) and ClustalW2 (http://www.ebi.ac.uk/Tools/msa/clustalw2; Larkin et al., 2007).

Screening Germplasm and Breeding Material for Drought Tolerance

A panel of 16 barley lines was screened for their yielding capacity under terminal drought (Supplemental Fig. S2). The plots subjected to terminal drought stress each comprised 50 plants and were randomly arranged in three replications. Well-watered control plots were also raised in parallel. A rainout shelter was installed over the droughted plots at anthesis, and 1 week later, irrigation was withheld until maturity. The following season, stay-green LP103 (variety QUENCH) and senescing LP110 (variety PASADENA) were regrown in a 10-replicate trial conducted in the same way as above. Grain yield per plot and thousand grain weight from both the irrigated and drought-stressed plants were obtained (at least 10 replicate plots per entry; Fig. 2C).

Production of Transgenic Material

Vector Construction

The barley *Lea B19.3* promoter (740 bp) was amplified from barley genomic DNA using *Lea* forward 5′-CCGTGTGCACATATACGAT-3′ and reverse 5′-TGCACGCTGCCTGGGACC-3′ primers and high-fidelity DNA Polymerase (Roche). *AtNCED6* was amplified with high-fidelity DNA Polymerase (Roche) from Arabidopsis genomic DNA (*NCED* genes lack introns) using gene-specific primers of *NCED6* (forward 5′-CCACCATGCAACACTCTCTTCGT-3′ and reverse 5′-GATCAGAAAACTTGTTCCTTCAAC-3′). The following PCR conditions were used: one cycle at 94°C (2 min), 30 cycles at 94°C (15 s), 56°C (30 s), and 72°C (2 min for *NCED6*, 1 min for *Lea* promoter), followed by extension at 72°C (7 min). Both amplified products were cloned into pCR4-TOPO vector (Invitrogen) and confirmed by sequencing. Using the TOPO clones as templates, the promoter region was amplified with primers containing *Pst*I and *Eco*RI restriction sites at the 5′ and 3′ end, respectively, and further cloned into pNOS-ABM vector (DNA Cloning Service) containing the *Agrobacterium tumefaciens nos* terminator downstream of the multiple cloning site used. *AtNCED6* coding region was amplified with gene-specific primers containing *Hind*III sites from the TOPO vector and subsequently cloned into *Lea*-pNOS1 (pNOS-ABM with *Lea* promoter). The complete expression cassette was excised using *Sfi*I restriction enzyme and cloned into the binary barley transformation vector p6U (DNA Cloning Service). Correct orientation was confirmed by sequencing.

For the repression of *HvABA8′OH-1* under control of *Lea B19.3* promoter, an RNAi approach was undertaken. First, *Lea* promoter was amplified with primers containing *Spe*I restriction sites and ligated into pNOS-ABM to create *Lea*-pNOS2. A 500-bp fragment of *HvABA8′OH-1* was amplified from the corresponding barley EST clone (HS06M03_contig211107) using primers *HvABA8′OH-1* forward 5′-TGCTCGAGTGGATGGTCAAGTTC-3′ and reverse 5′-TTCACTAGTAGGAAGACATAGAT-3′ with *Xho*I/*Spe*I restriction sites for the sense and *HvABA8′OH-1* forward 5′-TGGTCGACTGGATGGTCAAGTTC-3′ and reverse 5′-TTCGGATCCAGGAAGACATAGAT-3′ with *Sal*I/*Bam*HI restriction sites for the antisense fragment, respectively. The chosen fragment is placed in a rather conserved region of *HvABA8′OH-1*, so it is likely that all three *ABA8′OH* genes will be suppressed. Upon PCR amplification (one cycle at 94°C [2 min], 30 cycles at 94°C [15 s], 55°C [30 s], and 72°C [30 s], followed by extension at 72°C [7 min]), both amplified products were subcloned into the pAxi vector derived from pNOS-ABM through insertion of a 200-bp intron flanked by restriction sites. Correct clones were verified by sequencing. The RNAi cassette was subsequently excised from pAxi using *Pst*I/*Sal*I and ligated into *Lea*-pNOS2 (see above). The complete RNAi expression cassette was further excised using *Sfi*I restriction enzyme and cloned into p6U.

Transformation of Barley and Production of Homozygous Lines

Stable transformed barley plants (cv Golden Promise) were obtained by *A. tumefaciens*-mediated transformation following a protocol reported previously (Hensel et al., 2009). In brief, immature embryos were dissected from caryopses harvested 12 to 16 d after flowering. Upon inoculation and coculture with *A. tumefaciens* strain AGL-1 harboring an appropriate binary vector as specified above, the explants were grown on media supplemented with hygromycin to provide selective conditions. Rooted regenerants tested positive for the presence of the *hygromycin phosphotransferase* (*hpt*) gene were then established in soil and cultivated in a phytochamber providing 12-h daylength at 14°C/12°C day/night, respectively. At booting stage, the plants were transferred to a glasshouse cabin (16-h-light period, 18°C/16°C day/night, respectively) and grown until maturity.

For the pLea:NCED6 construct (*NCED6* overexpression), single-copy homozygous plants were identified by conventional segregation analysis across generations based on *hpt*-specific PCR and DNA gel blot. Two independent homozygous lines (T_3 generation) harboring a single insertion of the transgene were used for the experiments. For the pLea:ABA8′OH RNAi construct, doubled haploid plants were produced using embryogenic pollen cultures generated from primary transgenic plants following the protocol previously described by Coronado et al. (2005).

Growth Conditions of Transgenic and Breeding Material

For the experimental analyses, wild-type barley (cv Golden Promise) and homozygous transgenic plants (*pLea:NCED6* and *pLea:ABA8′OH RNAi*) were cultivated in a growth chamber (phytochamber) with a 16-h-light/8-h-dark cycle at 20°C/15°C, respectively. Spikes were labeled at anthesis, drought stress was imposed, and these plants were maintained at 10% soil moisture level by monitoring soil moisture using a moisture meter HH2 coupled with soil moisture sensor SM200 probes (Delta T Devices). Another batch of plants from a given experiment was continuously watered and treated as unstressed control. Two replications were maintained by growing them independently, and additional technical replications were maintained by the pool of samples collected from average of five plants. The flag leaves as well as first leaves were harvested from the wild type and transgenic lines at 2, 4, 8, and 12 DAS from stress and control plants. Imposition of stress took place at 4 d after flowering. These stages were chosen to cover short and long duration of stress. Material obtained from this batch of plants was used for measuring hormones, gene expression profiling, and various physiological experiments. As described above, the contrasting breeding material (stay-green and senescing plants) was cultivated, drought stress was imposed at 8 d after flowering, and flag leaf samples were harvested at 4, 8, 12, and 16 DAS.

Physiological Traits

Infrared gas analysis was carried out on individual fully emerged flag leaves of breeding material of stay green and senescing during 12 and 16 d after flowering (corresponding to 4 and 8 DAS) and flag leaf of transgenic and wild-type plant material during 4 DAS using a LC*pro*+ device (ADC Bioscientific). A constant supply of 400 μL L^{-1} CO_2 (flow rate, 200 μmol s^{-1}) was provided by a CO_2 cartridge and a photon flux density of 900 μmol m^{-2} s^{-1} by a mixed red/blue light-emitting diode light source mounted above the leaf chamber head. The net assimilation rate, internal CO_2 concentration, stomatal conductance, and transpiration rate were all recorded from five individual plants growing in both well-watered and drought-stressed conditions, with four technical replications per measurement. The measurements were only taken once the internal CO_2 concentration had stabilized (2–3 min after insertion of the leaf within the device). The instantaneous WUE was calculated from the ratio between the assimilation rate and the transpiration rate.

Phytohormone Measurements

The content of ABA and certain of its degradation products and Glc esters was measured along with that of cytokinin, gibberellins, and auxin hormone analysis. These were assessed by HPLC electrospray ionization-tandem mass spectrometry (carried out at the Plant Biotechnology Institute). The assays were calibrated using deuterated internal standards, as described elsewhere (Chiwocha et al., 2003; Kong et al., 2008).

qRT-PCR Analysis

RNA was isolated from breeding material as well from the wild type and transgenic lines from two independent biological replications and two technical replications (pooled from five plants) using the TRIzol reagent (Invitrogen) and RNAeasy columns (Qiagen). The RNA was converted to cDNA following Seiler et al. (2011). Gene-specific primers (targeting 25 ABA signaling genes) were designed using Primer Select software (DNAStar), and the relevant sequences are given in Supplemental Table S1. The reactions were performed in 384-well plates with an ABI PRISM 7900 HT Sequence Detection System (Applied Biosystems) using SYBR Green to monitor double-stranded DNA synthesis. For a more detailed protocol, see Seiler et al. (2011). The

amplification profile consisted of a denaturation step (50°C for 2 min, 95°C for 10 min), followed by 45 cycles of 95°C for 15 s and 60°C for 60 s. Amplicon dissociation curves were recorded after cycle 45 by heating from 60°C to 95°C with a ramp speed of 1.9°C min^{-1}. Data were collected from cycles 3 to 15 to generate a baseline-subtracted plot of the logarithmic increase in fluorescence signal versus cycle number, using SDS2.2.1 software (Applied Biosystems). A normalized reporter threshold of 0.2 was applied to obtain cycle threshold (C_T) values. To allow comparisons between different PCRs or templates, C_T values for each gene were normalized to the C_T value of the reference gene (elongation factor 1α, EST clone HZ42K12). PCR efficiency was calculated from the slope of the exponential phase of the amplification, following the suggestions made by Ramakers et al. (2003). Transcription levels are presented in the form $2^{-\Delta CT}$, where ΔC_T represents the difference between the C_T values of the target and the reference genes. Primer sequences can be found in Supplemental Table S1.

In transgenic barley plants, the mRNA expression levels of the *AtNCED6* gene and two *HvNCED* and three *HvABA8′OH* endogenous genes were monitored following gene specific primers: *AtNCED6* (forward 5′-GACAAAGGTTATGTAATGGGG-3′ and reverse 5′-CTTGTTCCTTCAACTGATTC-3′); *HvNCED1* (forward 5′-CCAGCACTAATCGATTCC-3′ and reverse 5′-GAGAGTGGTGATGAGTAA-3′); *HvNCED2* (forward 5′-CATGGAAAGAGGAAGTTG-3′ and reverse 5′-GAAGCAAGTGTGAGCTAAC-3′); *HvABA8′OH-1* (forward 5′-AGCACGGACCGTCAAAGTC-3′ and reverse 5′-TGAGAATGCCTACGTAGTG-3′); *HvABA8′OH-2* (forward 5′-GAGATGCTGGTGCTCATC-3′ and reverse 5′-ACGTCGTCGCTCGATCCAAC-3′); and *HvABA8′OH-3* (forward 5′-CCGGCGGCAGCGTCTTCT-3′ and reverse 5′-GTGTTGCCGTCCTGGGTGTCC-3′). qRT-PCR was performed as described above.

Y2H Assay

The full-length coding regions of barley *PYR/PYL1*, *PYR/PYL2*, *PYR/PYL5*, *PP2C4*, and *PKABA1/SnRK2.1* genes were initially cloned into pCR8/GW/TOPO TA vector (Invitrogen) and further introduced into pDEST22 (GAL4 activation domain, AD) and pDEST32 (GAL4 DNA binding domain, BD) vectors using GATEWAY technology following the manufacturer's instructions (ProQuest Two-Hybrid System with Gateway Technology, Invitrogen). Clones containing the *PP2C4 (AD)*, *PP2C4 (BD)*, *PYR/PYL1 (AD)*, *PYR/PYL1 (BD)*, *PYR/PYL2 (AD)*, *PYR/PYL2 (BD)*, *PYR/PYL5 (AD)*, *PYR/PYL5 (BD)*, *PKABA1/SnRK2.1 (AD)*, and *PKABA1/SnRK2.1 (BD)* fusions were validated by sequence analysis and subsequently used in the Y2H assay. Specific combinations of activation domain and binding domain plasmids were cotransformed into the yeast (*Saccharomyces cerevisiae*) strain MaV203 (*MATα*; *leu2-3,112*; *trp1-901*; *his3Δ200*; *ade2-101*; *gal4Δ*; *gal80Δ*; $SPAL10_{UASGAL1}$::*URA3*; *GAL1*::*lacZ*; $HIS3_{UASGAL1}$::*HIS3@LYS2*; $can1^R$; $cyh2^R$), using a lithium acetate/polyethylene glycol protocol described by Gietz and Woods (2006), and the transformed cells were spread on synthetic complete (SC)-Leu-Trp media plates. Autoactivation levels of yeast transformants harboring *PP2C4 (BD)*, *PYR/PYL1 (BD)*, *PYR/PYL2 (BD)*, *PYR/PYL5 (BD)*, and *PKABA1/SnRK2.1 (BD)* were determined using synthetic dextrose medium lacking Leu and His (–leu, –his), to which 0, 10, 25, 50, 75, or 100 mM of the His biosynthesis inhibitor 3-amino-1,2,4-triazole (3-AT) was added (Durfee et al., 1993). Interactions were determined by growth of double yeast colonies on to three selective medium plates: SC-Leu-Trp, SC-Leu-Trp-His plus 50 mm 3-AT, and SC-Leu-Trp-His plus 50 mm 3-AT and 100 μM ABA (mixed stereoisomers, Sigma). The empty vectors pDEST22, pDEST32, Krev1, RalGDS-wt, RalGDS-m1, or RalGDS-m2 were cotransformed as positive and negative controls as mentioned in the manufacturer's instructions. The selection plates were incubated at 30°C, and growth of the colonies was assessed after 3 d. The screening experiment was performed in triplicate.

BiFC Analysis and Transient Gene Expression in Arabidopsis Protoplasts

HvPP2C4 was cloned into the pSPYNE vector, which contains the N-terminal 155 amino acids of YFP, and *HvPYR/PYL* genes were cloned into the pSPYCE vector, containing the C-terminal 86 amino acids of YFP. To test for dimer formation, *HvPYR/PYL* genes were additionally cloned into pSPYNE vector. To check interaction of PP2C4 with PKABA1/SnRK2.1 of the SnRK2 family, *HvPKABA1/SnRK2.1* and *HvPP2C4* were cloned into pSPYCE and pSPYNE vectors, respectively. Combinations of BiFC constructs were cotransformed into Arabidopsis protoplasts and fluorescence was detected.

PYR/PYL1, *PYR/PYL2*, *PYR/PYL5*, *PP2C4*, and *PKABA1/SnRK2.1* in pCR8/GW/TOPO TA vector (previous section) were subsequently recombined via an LR recombination into the binary plant transformation vectors pSPYNE and pSPYCE (Walter et al., 2004), resulting in fusion with the N- or C-terminal portion of the YFP sequence, respectively. Arabidopsis protoplast isolation and transient expression assays were performed as described in Yoo et al. (2007. Plants were grown in soil under short-day conditions (8-h light/16-h dark at 20°C and 18°C, respectively) for 4 weeks. Freshly isolated leaf mesophyll protoplasts (0.5 mL) were cotransfected with various pairs of plasmid DNA (pSPYNE/pSPYCE) and pUGW15-CFP, which was used as transformation control (Nakagawa et al., 2007). The total amount of DNA was 50 μg in 1:1:1 ratio. YFP fluorescence was evaluated 1 d after transfection (incubation in dark) using the LSM 710 Laser Scanning System (Zeiss). To investigate a possible ABA response, 5 μM ABA (mixed stereoisomers, Sigma) was applied after transfection and then additionally incubated for 1 h at room temperature. For stress treatment, protoplasts were centrifuged at 200*g* for 1 min and suspended in media (Yoo et al., 2007) containing 10% (w/v) polyethylene glycol or 800 mM mannitol, respectively, followed by 1 h incubation at room temperature.

Molecular Modeling of Barley PYR/PYLs

The three-dimensional models of the complete amino acid sequence of barley HvPYR/PYL1, HvPYR/PYL2, and HvPYR/PYL5 were created by the I-TASSER server (Roy et al., 2010). From the proposed models, we selected the one with best scores, downloaded structural overlays with Arabidopsis analogs, predicted ligand-binding sites from the I-TASSER server, and further processed it by using the PyMOL Software (The PyMOL Molecular Graphics System, Version 1.3, Schrödinger). The complete results including coordinates of the models along with *Z*-score significance could be searched at I-Tasser database (http://zhanglab.ccmb.med.umich.edu/I-TASSER/search.html) with the following identifications for HvPYR/PYL1 (S91589), HvPYR/PYL2 (S91695), and HvPYR/PYL5 (S91499).

Statistical Analysis

Values derived from several biological replicates were used to calculate standard deviations, and statistical significance was assessed using the Student's *t* test and one-way ANOVA across genotypes for a given treatment at $\alpha = 0.05$ or 0.01 with Tukey's posthoc test using the SPSS software package (IBM). In addition, two-way ANOVA was also performed to identify the signified difference between accessions (stay-green versus senescing line; wild type versus transgenic lines) and condition (control versus drought stress) with *P* values of the *f*-test. Letters a, b, and c and x, y, and z represent statistical differences across genotypes under control and stress conditions, respectively. Bars with similar or no letters indicate no statistical difference among genotypes under a given treatment.

Supplemental Data

The following materials are available in the online version of this article.

Supplemental Figure S1. Amino acid sequence alignment of the Arabidopsis PYR1/RCAR11 protein with putative barley PYR/PYL orthologous proteins, barley and Arabidopsis PP2Cs, and the Arabidopsis SnRK2.2, SnRK2.3, and SnRK2.6 proteins with barley SnRK2 orthologous proteins.

Supplemental Figure S2. Field screening of different barley lines.

Supplemental Figure S3. Differential expression of putative ABA biosynthesis, degradation, and deconjugation genes in two barley contrasting genotypes under terminal drought stress analyzed by qRT-PCR.

Supplemental Figure S4. ABA, ABA metabolites, and differential expression of putative ABA signaling genes in two barley contrasting genotypes under terminal drought stress.

Supplemental Figure S5. Relative expression levels of barley endogenous genes *HvNCED1*, *HvNCED2*, and *ABA8′OH1-3*.

Supplemental Figure S6. Differential expression of putative ABA signaling genes in barley wild type and transgenic plants under terminal drought stress analyzed by qRT-PCR.

Supplemental Figure S7. Interaction of ABA receptor components using different stress treatments analyzed by BiFC.

Supplemental Table S1. List of genes putatively involved in ABA signaling/biosynthesis and primer sequences used for qRT-PCR.

Supplemental Table S2. Levels of ABA, ABA metabolites, and other hormones in flag leaf and seeds under control and stress conditions at 8 DAS.

Supplemental Table S3. Statistically significant differences in expression of ABA biosynthesis and signaling genes between contrasting breeding lines.

Supplemental Table S4. Statistically significant differences in expression of ABA biosynthesis and signaling genes between genotypes, ABA metabolites, and physiological traits of transgenics.

ACKNOWLEDGMENTS

We thank Jana Lorenz and Gabriele Einert (Leibniz Institute of Plant Genetics and Crop Plant Research [IPK]) for their excellent technical assistance, Cornelia Marthe, Andrea Müller, and Ingrid Otto (IPK) for their excellent technical assistance in generating transgenic barley plants and doubled haploids, Dr. Irina Zaharia (National Research Council of Canada, Plant Biotechnology Institute) for hormone measurements, Dr. Uwe Scholz (IPK) for performing the BLAST analysis, Dr. Nils Stein (IPK) for providing access to Whole Genome Shotgun sequencing of barley, and Roslen Anacleto (International Rice Research Institute) for statistical assistance.

Received September 22, 2013; accepted February 25, 2014; published March 7, 2014.

LITERATURE CITED

Aswath CR, Kim SH, Mo SY, Kim DH (2005) Transgenic plants of creeping bent grass harboring the stress inducible gene, 9-cis-epoxycarotenoid dioxygenase, are highly tolerant to drought and NaCl stress. Plant Growth Regul **47:** 129–139

Belin C, de Franco PO, Bourbousse C, Chaignepain S, Schmitter JM, Vavasseur A, Giraudat J, Barbier-Brygoo H, Thomine S (2006) Identification of features regulating OST1 kinase activity and OST1 function in guard cells. Plant Physiol **141:** 1316–1327

Ben-Ari G (2012) The ABA signal transduction mechanism in commercial crops: learning from Arabidopsis. Plant Cell Rep **31:** 1357–1369

Blum A (1996) Crop responses to drought and the interpretation of adaptation. Plant Growth Regul **20:** 135–148

Boneh U, Biton I, Zheng C, Schwartz A, Ben-Ari G (2012) Characterization of potential ABA receptors in *Vitis vinifera*. Plant Cell Rep **31:** 311–321

Bork P, Brown NP, Hegyi H, Schultz J (1996) The protein phosphatase 2C (PP2C) superfamily: detection of bacterial homologues. Protein Sci **5:** 1421–1425

Boudsocq M, Barbier-Brygoo H, Laurière C (2004) Identification of nine sucrose nonfermenting 1-related protein kinases 2 activated by hyperosmotic and saline stresses in *Arabidopsis thaliana*. J Biol Chem **279:** 41758–41766

Boyer JS, Westgate ME (2004) Grain yields with limited water. J Exp Bot **55:** 2385–2394

Chan Z (2012) Expression profiling of ABA pathway transcripts indicates crosstalk between abiotic and biotic stress responses in Arabidopsis. Genomics **100:** 110–115

Chen J, Chang SX, Anyia AO (2011) Gene discovery in cereals through quantitative trait loci and expression analysis in water-use efficiency measured by carbon isotope discrimination. Plant Cell Environ **34:** 2009–2023

Chiwocha SD, Abrams SR, Ambrose SJ, Cutler AJ, Loewen M, Ross AR, Kermode AR (2003) A method for profiling classes of plant hormones and their metabolites using liquid chromatography-electrospray ionization tandem mass spectrometry: an analysis of hormone regulation of thermodormancy of lettuce (*Lactuca sativa* L.) seeds. Plant J **35:** 405–417

Christmann A, Weiler EW, Steudle E, Grill E (2007) A hydraulic signal in root-to-shoot signalling of water shortage. Plant J **52:** 167–174

Condon AG, Richards RA (1992) Broad sense heritability and genotype × environment interaction for carbon isotope discrimination in field-grown wheat. Aust J Agric Res **43:** 921–934

Coronado MJ, Hensel G, Broeders S, Otto I, Kumlehn J (2005) Immature pollen-derived doubled haploid formation in barley cv Golden Promise as a tool for transgene recombination. Acta Physiol Plant **27:** 591–599

Cutler AJ, Krochko JE (1999) Formation and breakdown of ABA. Trends Plant Sci **4:** 472–478

Cutler SR, Rodriguez PL, Finkelstein RR, Abrams SR (2010) Abscisic acid: emergence of a core signaling network. Annu Rev Plant Biol **61:** 651–679

Dupeux F, Santiago J, Betz K, Twycross J, Park SY, Rodriguez L, Gonzalez-Guzman M, Jensen MR, Krasnogor N, Blackledge M, et al (2011) A thermodynamic switch modulates abscisic acid receptor sensitivity. EMBO J **30:** 4171–4184

Durfee T, Becherer K, Chen PL, Yeh SH, Yang Y, Kilburn AE, Lee WH, Elledge SJ (1993) The retinoblastoma protein associates with the protein phosphatase type 1 catalytic subunit. Genes Dev **7:** 555–569

Fujii H, Chinnusamy V, Rodrigues A, Rubio S, Antoni R, Park SY, Cutler SR, Sheen J, Rodriguez PL, Zhu JK (2009) In vitro reconstitution of an abscisic acid signalling pathway. Nature **462:** 660–664

Gietz RD, Woods RA (2006) Yeast transformation by the LiAc/SS Carrier DNA/PEG method. Methods Mol Biol **313:** 107–120

Gittins JR, Pellny TK, Hiles ER, Rosa C, Biricolti S, James DJ (2000) Transgene expression driven by heterologous ribulose-1,5-bisphosphate carboxylase/oxygenase small-subunit gene promoters in the vegetative tissues of apple (*Malus pumila* mill.). Planta **210:** 232–240

Gubler F, Hughes T, Waterhouse P, Jacobsen J (2008) Regulation of dormancy in barley by blue light and after-ripening: effects on abscisic acid and gibberellin metabolism. Plant Physiol **147:** 886–896

Hall NM, Griffiths H, Corlett JA, Jones HG, Lynn J, King GJ (2005) Relationships between water-use traits and photosynthesis in *Brassica oleracea* resolved by quantitative genetic analysis. Plant Breed **124:** 557–564

Hensel G, Kastner C, Oleszczuk S, Riechen J, Kumlehn J (2009) *Agrobacterium*-mediated gene transfer to cereal crop plants: current protocols for barley, wheat, triticale, and maize. Int J Plant Genomics **2009:** 835608

Hubbard KE, Nishimura N, Hitomi K, Getzoff ED, Schroeder JI (2010) Early abscisic acid signal transduction mechanisms: newly discovered components and newly emerging questions. Genes Dev **24:** 1695–1708

Iuchi S, Kobayashi M, Taji T, Naramoto M, Seki M, Kato T, Tabata S, Kakubari Y, Yamaguchi-Shinozaki K, Shinozaki K (2001) Regulation of drought tolerance by gene manipulation of 9-cis-epoxycarotenoid dioxygenase, a key enzyme in abscisic acid biosynthesis in Arabidopsis. Plant J **27:** 325–333

Iyer LM, Koonin EV, Aravind L (2001) Adaptations of the helix-grip fold for ligand binding and catalysis in the START domain superfamily. Proteins **43:** 134–144

Ji XM, Dong BD, Shiran B, Talbot MJ, Edlington JE, Hughes T, White RG, Gubler F, Dolferus R (2011) Control of abscisic acid catabolism and abscisic acid homeostasis is important for reproductive stage stress tolerance in cereals. Plant Physiol **156:** 647–662

Juenger TE, Mckay JK, Hausmann N, Keurentjes JJB, Sen S, Stowe KA, Dawson TE, Simms EL, Richards JH (2005) Identification and characterization of QTL underlying whole-plant physiology in *Arabidopsis thaliana*: δC-13, stomatal conductance and transpiration efficiency. Plant Cell Environ **28:** 697–708

Karaba A, Dixit S, Greco R, Aharoni A, Trijatmiko KR, Marsch-Martinez N, Krishnan A, Nataraja KN, Udayakumar M, Pereira A (2007) Improvement of water use efficiency in rice by expression of *HARDY*, an Arabidopsis drought and salt tolerance gene. Proc Natl Acad Sci USA **104:** 15270–15275

Kim H, Hwang H, Hong JW, Lee YN, Ahn IP, Yoon IS, Yoo SD, Lee S, Lee SC, Kim BG (2012) A rice orthologue of the ABA receptor, OsPYL/RCAR5, is a positive regulator of the ABA signal transduction pathway in seed germination and early seedling growth. J Exp Bot **63:** 1013–1024

Kline KG, Sussman MR, Jones AM (2010) Abscisic acid receptors. Plant Physiol **154:** 479–482

Klingler JP, Batelli G, Zhu JK (2010) ABA receptors: the START of a new paradigm in phytohormone signalling. J Exp Bot **61:** 3199–3210

Kong L, Abrams SR, Owen SJ, Graham H, von Aderkas P (2008) Phytohormones and their metabolites during long shoot development in Douglas fir following cone induction by gibberellin injection. Tree Physiol **28:** 1357–1364

Larkin MA, Blackshields G, Brown NP, Chenna R, McGettigan PA, McWilliam H, Valentin F, Wallace IM, Wilm A, Lopez R, et al (2007) Clustal W and Clustal X version 2.0. Bioinformatics **23:** 2947–2948

Ma Y, Szostkiewicz I, Korte A, Moes D, Yang Y, Christmann A, Grill E (2009) Regulators of PP2C phosphatase activity function as abscisic acid sensors. Science **324:** 1064–1068

Masle J, Gilmore SR, Farquhar GD (2005) The *ERECTA* gene regulates plant transpiration efficiency in Arabidopsis. Nature **436:** 866–870

Matsumoto T, Tanaka T, Sakai H, Amano N, Kanamori H, Kurita K, Kikuta A, Kamiya K, Yamamoto M, Ikawa H, et al (2011) Comprehensive sequence analysis of 24,783 barley full-length cDNAs derived from 12 clone libraries. Plant Physiol **156:** 20–28

McCourt P, Creelman R (2008) The ABA receptors: we report you decide. Curr Opin Plant Biol **11:** 474–478

Melcher K, Ng LM, Zhou XE, Soon FF, Xu Y, Suino-Powell KM, Park SY, Weiner JJ, Fujii H, Chinnusamy V, et al (2009) A gate-latch-lock mechanism for hormone signalling by abscisic acid receptors. Nature **462:** 602–608

Merilo E, Laanemets K, Hu HH, Xue SW, Jakobson L, Tulva I, Gonzalez-Guzman M, Rodriguez PL, Schroeder JI, Broschè M, et al (2013) PYR/RCAR receptors contribute to ozone-, reduced air humidity-, darkness-, and CO_2-induced stomatal regulation. Plant Physiol **162:** 1652–1668

Millar AA, Jacobsen JV, Ross JJ, Helliwell CA, Poole AT, Scofield G, Reid JB, Gubler F (2006) Seed dormancy and ABA metabolism in Arabidopsis and barley: the role of ABA 8′-hydroxylase. Plant J **45:** 942–954

Miyakawa T, Fujita Y, Yamaguchi-Shinozaki K, Tanokura M (2013) Structure and function of abscisic acid receptors. Trends Plant Sci **18:** 259–266

Miyazono KI, Miyakawa T, Sawano Y, Kubota K, Kang HJ, Asano A, Miyauchi Y, Takahashi M, Zhi Y, Fujita Y, et al (2009) Structural basis of abscisic acid signalling. Nature **462:** 609–614

Nakagawa T, Kurose T, Hino T, Tanaka K, Kawamukai M, Niwa Y, Toyooka K, Matsuoka K, Jinbo T, Kimura T (2007) Development of series of gateway binary vectors, pGWBs, for realizing efficient construction of fusion genes for plant transformation. J Biosci Bioeng **104:** 34–41

Okamoto M, Peterson FC, Defries A, Park SY, Endo A, Nambara E, Volkman BF, Cutler SR (2013) Activation of dimeric ABA receptors elicits guard cell closure, ABA-regulated gene expression, and drought tolerance. Proc Natl Acad Sci USA **110:** 12132–12137

Park SY, Fung P, Nishimura N, Jensen DR, Fujii H, Zhao Y, Lumba S, Santiago J, Rodrigues A, Chow TF, et al (2009) Abscisic acid inhibits type 2C protein phosphatases via the PYR/PYL family of START proteins. Science **324:** 1068–1071

Pizzio GA, Rodriguez L, Antoni R, Gonzalez-Guzman M, Yunta C, Merilo E, Kollist H, Albert A, Rodriguez PL (2013) The PYL4 A194T mutant uncovers a key role of PYR1-LIKE4/PROTEIN PHOSPHATASE 2CA interaction for abscisic acid signaling and plant drought resistance. Plant Physiol **163:** 441–455

Qin X, Zeevaart JA (2002) Overexpression of a 9-cis-epoxycarotenoid dioxygenase gene in *Nicotiana plumbaginifolia* increases abscisic acid and phaseic acid levels and enhances drought tolerance. Plant Physiol **128:** 544–551

Radauer C, Lackner P, Breiteneder H (2008) The Bet v 1 fold: an ancient, versatile scaffold for binding of large, hydrophobic ligands. BMC Evol Biol **8:** 286

Raghavendra AS, Gonugunta VK, Christmann A, Grill E (2010) ABA perception and signalling. Trends Plant Sci **15:** 395–401

Ramakers C, Ruijter JM, Deprez RH, Moorman AF (2003) Assumption-free analysis of quantitative real-time polymerase chain reaction (PCR) data. Neurosci Lett **339:** 62–66

Rebetzke GJ, Condon AG, Richards RA, Farquhar GD (2002) Selection for reduced carbon isotope discrimination increases aerial biomass and grain yield of rainfed bread wheat. Crop Sci **42:** 739–745

Richards RA (1996) Defining selection criteria to improve yield under drought. Plant Growth Regul **20:** 157–166

Richards RA, Rebetzke GJ, Condon AG, van Herwaarden AF (2002) Breeding opportunities for increasing the efficiency of water use and crop yield in temperate cereals. Crop Sci **42:** 111–121

Romero P, Lafuente MT, Rodrigo MJ (2012) The Citrus ABA signalosome: identification and transcriptional regulation during sweet orange fruit ripening and leaf dehydration. J Exp Bot **63:** 4931–4945

Roy A, Kucukural A, Zhang Y (2010) I-TASSER: a unified platform for automated protein structure and function prediction. Nat Protoc **5:** 725–738

Santiago J, Dupeux F, Betz K, Antoni R, Gonzalez-Guzman M, Rodriguez L, Márquez JA, Rodriguez PL (2012) Structural insights into PYR/PYL/RCAR ABA receptors and PP2Cs. Plant Sci **182:** 3–11

Santiago J, Dupeux F, Round A, Antoni R, Park SY, Jamin M, Cutler SR, Rodriguez PL, Márquez JA (2009a) The abscisic acid receptor PYR1 in complex with abscisic acid. Nature **462:** 665–668

Santiago J, Rodrigues A, Saez A, Rubio S, Antoni R, Dupeux F, Park SY, Márquez JA, Cutler SR, Rodriguez PL (2009b) Modulation of drought resistance by the abscisic acid receptor PYL5 through inhibition of clade A PP2Cs. Plant J **60:** 575–588

Seiler C, Harshavardhan VT, Rajesh K, Reddy PS, Strickert M, Rolletschek H, Scholz U, Wobus U, Sreenivasulu N (2011) ABA biosynthesis and degradation contributing to ABA homeostasis during barley seed development under control and terminal drought-stress conditions. J Exp Bot **62:** 2615–2632

Sreenivasulu N, Harshavardhan VT, Govind G, Seiler C, Kohli A (2012) Contrapuntal role of ABA: does it mediate stress tolerance or plant growth retardation under long-term drought stress? Gene **506:** 265–273

Sreenivasulu N, Sopory SK, Kavi Kishor PB (2007) Deciphering the regulatory mechanisms of abiotic stress tolerance in plants by genomic approaches. Gene **388:** 1–13

Sun L, Wang YP, Chen P, Ren J, Ji K, Li Q, Li P, Dai SJ, Leng P (2011) Transcriptional regulation of SlPYL, SlPP2C, and SlSnRK2 gene families encoding ABA signal core components during tomato fruit development and drought stress. J Exp Bot **62:** 5659–5669

Szostkiewicz I, Richter K, Kepka M, Demmel S, Ma Y, Korte A, Assaad FF, Christmann A, Grill E (2010) Closely related receptor complexes differ in their ABA selectivity and sensitivity. Plant J **61:** 25–35

Teulat B, Merah O, Sirault X, Borries C, Waugh R, This D (2002) QTLs for grain carbon isotope discrimination in field-grown barley. Theor Appl Genet **106:** 118–126

Thomas H, Howarth CJ (2000) Five ways to stay green. J Exp Bot **51:** 329–337

Thompson AJ, Jackson AC, Symonds RC, Mulholland BJ, Dadswell AR, Blake PS, Burbidge A, Taylor IB (2000) Ectopic expression of a tomato 9-cis-epoxycarotenoid dioxygenase gene causes over-production of abscisic acid. Plant J **23:** 363–374

Tung SA, Smeeton R, White CA, Black CR, Taylor IB, Hilton HW, Thompson AJ (2008) Over-expression of *LeNCED1* in tomato (*Solanum lycopersicum* L.) with the *rbcS3C* promoter allows recovery of lines that accumulate very high levels of abscisic acid and exhibit severe phenotypes. Plant Cell Environ **31:** 968–981

Umezawa T, Okamoto M, Kushiro T, Nambara E, Oono Y, Seki M, Kobayashi M, Koshiba T, Kamiya Y, Shinozaki K (2006) CYP707A3, a major ABA 8′-hydroxylase involved in dehydration and rehydration response in *Arabidopsis thaliana*. Plant J **46:** 171–182

Umezawa T, Nakashima K, Miyakawa T, Kuromori T, Tanokura M, Shinozaki K, Yamaguchi-Shinozaki K (2010) Molecular basis of the core regulatory network in ABA responses: sensing, signaling and transport. Plant Cell Physiol **51:** 1821–1839

Umezawa T, Sugiyama N, Mizoguchi M, Hayashi S, Myouga F, Yamaguchi-Shinozaki K, Ishihama Y, Hirayama T, Shinozaki K (2009) Type 2C protein phosphatases directly regulate abscisic acid-activated protein kinases in Arabidopsis. Proc Natl Acad Sci USA **106:** 17588–17593

Vlad F, Rubio S, Rodrigues A, Sirichandra C, Belin C, Robert N, Leung J, Rodriguez PL, Laurière C, Merlot S (2009) Protein phosphatases 2C regulate the activation of the Snf1-related kinase OST1 by abscisic acid in *Arabidopsis*. Plant Cell **21:** 3170–3184

Walter M, Chaban C, Schütze K, Batistic O, Weckermann K, Näke C, Blazevic D, Grefen C, Schumacher K, Oecking C, et al (2004) Visualization of protein interactions in living plant cells using bimolecular fluorescence complementation. Plant J **40:** 428–438

Yamauchi D, Zentella R, Ho TH (2002) Molecular analysis of the barley (*Hordeum vulgare* L.) gene encoding the protein kinase PKABA1 capable of suppressing gibberellin action in aleurone layers. Planta **215:** 319–326

Yang SH, Zeevaart JA (2006) Expression of *ABA 8′-hydroxylases* in relation to leaf water relations and seed development in bean. Plant J **47:** 675–686

Yin P, Fan H, Hao Q, Yuan X, Wu D, Pang Y, Yan C, Li W, Wang J, Yan N (2009) Structural insights into the mechanism of abscisic acid signaling by PYL proteins. Nat Struct Mol Biol **16:** 1230–1236

Yoo CY, Pence HE, Jin JB, Miura K, Gosney MJ, Hasegawa PM, Mickelbart MV (2010) The *Arabidopsis* GTL1 transcription factor regulates water use efficiency and drought tolerance by modulating stomatal density via transrepression of SDD1. Plant Cell **22:** 4128–4141

Yoo SD, Cho YH, Sheen J (2007) Arabidopsis mesophyll protoplasts: a versatile cell system for transient gene expression analysis. Nat Protoc **2:** 1565–1572

Yoshida R, Umezawa T, Mizoguchi T, Takahashi S, Takahashi F, Shinozaki K (2006) The regulatory domain of SRK2E/OST1/SnRK2.6 interacts with ABI1 and integrates abscisic acid (ABA) and osmotic stress signals controlling stomatal closure in Arabidopsis. J Biol Chem **281:** 5310–5318

Zhao Y, Chan Z, Xing L, Liu X, Hou YJ, Chinnusamy V, Wang P, Duan C, Zhu JK (2013) The unique mode of action of a divergent member of the ABA-receptor protein family in ABA and stress signaling. Cell Res **23:** 1380–1395

Zhengbin Z, Ping X, Hongbo S, Mengjun L, Zhenyan F, Liye C (2011) Advances and prospects: biotechnologically improving crop water use efficiency. Crit Rev Biotechnol **31:** 281–293

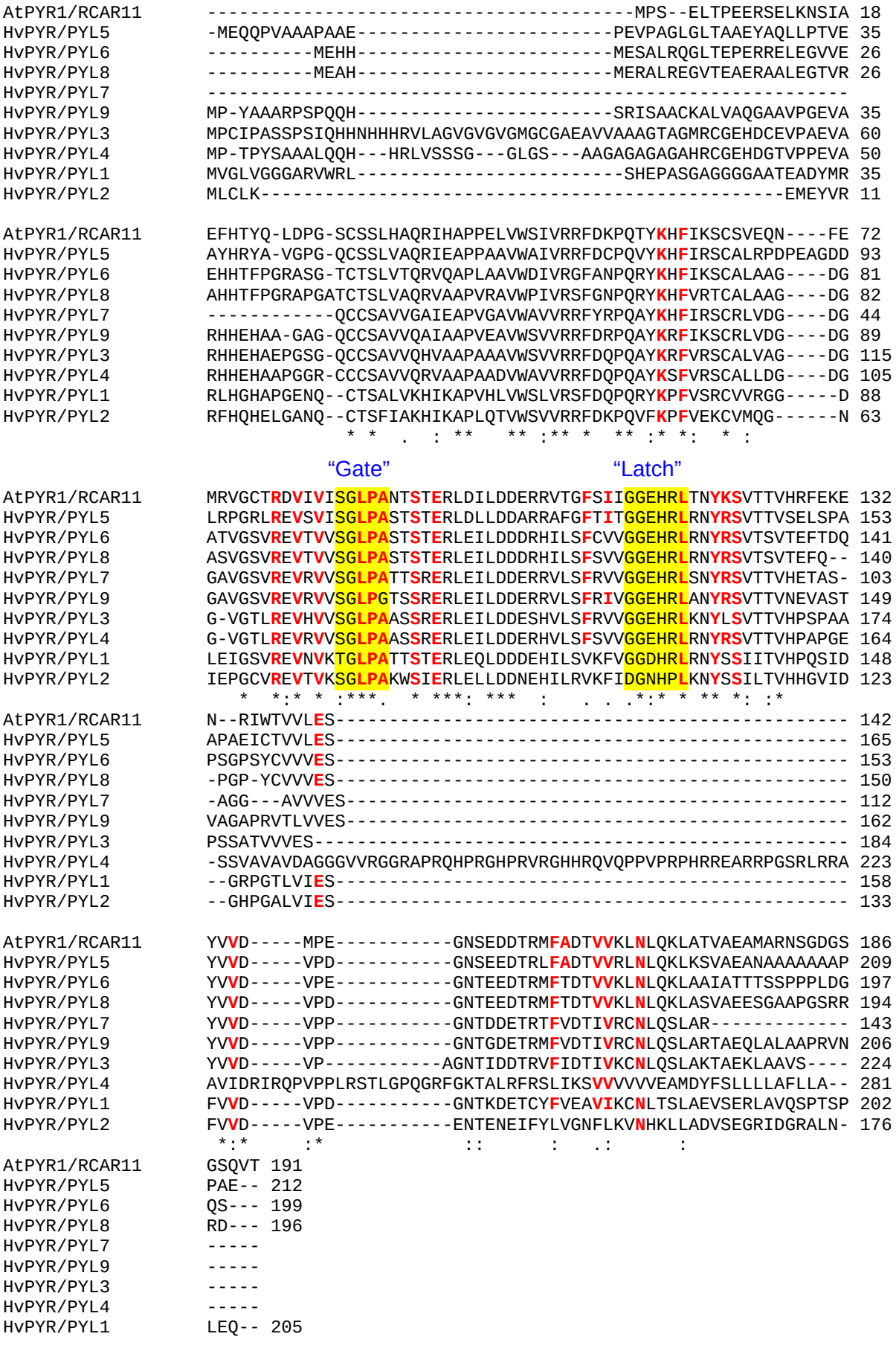
AtPYR1/RCAR11 ----------MPS--ELTPEERSELKNSIA 18
HvPYR/PYL5 -MEQQPVAAAPAAE----------PEVPAGLGLTAAEYAQLLPTVE 35
HvPYR/PYL6 ----------MEHH----------MESALRQGLTEPERRELEGVVE 26
HvPYR/PYL8 ----------MEAH----------MERALREGVTEAERAALEGTVR 26
HvPYR/PYL7 ----------
HvPYR/PYL9 MP-YAAARPSPQQH----------SRISAACKALVAQGAAVPGEVA 35
HvPYR/PYL3 MPCIPASSPSIQHHNHHHRVLAGVGVGVGMGCGAEAVVAAAGTAGMRCGEHDCEVPAEVA 60
HvPYR/PYL4 MP-TPYSAAALQQH---HRLVSSSG---GLGS---AAGAGAGAGAHRCGEHDGTVPPEVA 50
HvPYR/PYL1 MVGLVGGGARVWRL----------SHEPASGAGGGGAATEADYMR 35
HvPYR/PYL2 MLCLK----------EMEYVR 11
AtPYR1/RCAR11 EFHTYQ-LDPG-SCSSLHAQRIHAPPELVWSIVRRFDKPQTYKHFIKSCSVEQN----FE 72
HvPYR/PYL5 AYHRYA-VGPG-QCSSLVAQRIEAPPAAVWAIVRRFDCPQVYKHFIRSCALRPDPEAGDD 93
HvPYR/PYL6 EHHTFPGRASG-TCTSLVTQRVQAPLAAVWDIVRGFANPQRYKHFIKSCALAAG----DG 81
HvPYR/PYL8 AHHTFPGRAPGATCTSLVAQRVAAPVRAVWPIVRSFGNPQRYKHFVRTCALAAG----DG 82
HvPYR/PYL7 ----------QCCSAVVGAIEAPVGAVWAVVRRFYRPQAYKHFIRSCRLVDG----DG 44
HvPYR/PYL9 RHHEHAA-GAG-QCCSAVVQAIAAPVEAVWSVVRRFDRPQAYKRFIKSCRLVDG----DG 89
HvPYR/PYL3 RHHEHAEPGSG-QCCSAVVQHVAAPAAAVWSVVRRFDQPQAYKRFVRSCALVAG----DG 115
HvPYR/PYL4 RHHEHAAPGGR-CCCSAVVQRVAAPAADVWAVVRRFDQPQAYKSFVRSCALLDG----DG 105
HvPYR/PYL1 RLHGHAPGENQ--CTSALVKHIKAPVHLVWSLVRSFDQPQRYKPFVSRCVVRGG-----D 88
HvPYR/PYL2 RFHQHELGANQ--CTSFIAKHIKAPLQTVWSVVRRFDKPQVFKPFVEKCVMQG------N 63
"Gate"
"Latch"
AtPYR1/RCAR11 MRVGCTRDVIVISGLPANTSTERLDILDDERRVTGFSIIGGEHRLTNYKSVTTVHRFEKE 132
HvPYR/PYL5 LRPGRLREVSVISGLPASTSTERLDLLDDARRAFGFTITGGEHRLRNYRSVTTVSELSPA 153
HvPYR/PYL6 ATVGSVREVTVVSGLPASTSTERLEILDDDRHILSFCVVGGEHRLRNYRSVTSVTEFTDQ 141
HvPYR/PYL8 ASVGSVREVTVVSGLPASTSTERLEILDDDRHILSFSVVGGEHRLRNYRSVTSVTEFQ-- 140
HvPYR/PYL7 GAVGSVREVRVVSGLPATTSRERLEILDDERRVLSFRVVGGEHRLSNYRSVTTVHETAS- 103
HvPYR/PYL9 GAVGSVREVRVVSGLPGTSSRERLEILDDERRVLSFRIVGGEHRLANYRSVTTVNEVAST 149
HvPYR/PYL3 G-VGTLREVHVVSGLPAASSRERLEILDDESHVLSFRVVGGEHRLKNYLSVTTVHPSPAA 174
HvPYR/PYL4 G-VGTLREVRVVSGLPAASSRERLEILDDERHVLSFSVVGGEHRLRNYRSVTTVHPAPGE 164
HvPYR/PYL1 LEIGSVREVNVKTGLPATTSTERLEQLDDDEHILSVKFVGGDHRLRNYSSIITVHPQSID 148
HvPYR/PYL2 IEPGCVREVTVKSGLPAKWSIERLELLDDNEHILRVKFIDGNHPLKNYSSILTVHHGVID 123
AtPYR1/RCAR11 N--RIWTVVLES---------- 142
HvPYR/PYL5 APAEICTVVLES---------- 165
HvPYR/PYL6 PSGPSYCVVVES---------- 153
HvPYR/PYL8 -PGP-YCVVVES---------- 150
HvPYR/PYL7 -AGG---AVVVES---------- 112
HvPYR/PYL9 VAGAPRVTLVVES---------- 162
HvPYR/PYL3 PSSATVVVES---------- 184
HvPYR/PYL4 -SSVAVAVDAGGGVVRGGRAPRQHPRGHPRVRGHHRQVQPPVPRPHRREARRPGSRLRRA 223
HvPYR/PYL1 --GRPGTLVIES---------- 158
HvPYR/PYL2 --GHPGALVIES---------- 133
AtPYR1/RCAR11 YVVD-----MPE----------GNSEDDTRMFADTVVKLNLQKLATVAEAMARNSGDGS 186
HvPYR/PYL5 YVVD-----VPD----------GNSEEDTRLFADTVVRLNLQKLKSVAEANAAAAAAAP 209
HvPYR/PYL6 YVVD-----VPE----------GNTEEDTRMFTDTVVKLNLQKLAAIATTTSSPPPLDG 197
HvPYR/PYL8 YVVD-----VPD----------GNTEEDTRMFTDTVVKLNLQKLASVAEESGAAPGSRR 194
HvPYR/PYL7 YVVD-----VPP----------GNTDDETRTFVDTIVRCNLQSLAR---------- 143
HvPYR/PYL9 YVVD-----VPP----------GNTGDETRMFVDTIVRCNLQSLARTAEQLALAAPRVN 206
HvPYR/PYL3 YVVD-----VP----------AGNTIDDTRVFIDTIVKCNLQSLAKTAEKLAAVS---- 224
HvPYR/PYL4 AVIDRIRQPVPPLRSTLGPQGRFGKTALRFRSLIKSVVVVVVEAMDYFSLLLLAFLLA-- 281
HvPYR/PYL1 FVVD-----VPD----------GNTKDETCYFVEAVIKCNLTSLAEVSERLAVQSPTSP 202
HvPYR/PYL2 FVVD-----VPE----------ENTENEIFYLVGNFLKVNHKLLADVSEGRIDGRALN- 176
AtPYR1/RCAR11 GSQVT 191
HvPYR/PYL5 PAE-- 212
HvPYR/PYL6 QS--- 199
HvPYR/PYL8 RD--- 196
HvPYR/PYL7 -----
HvPYR/PYL9 -----
HvPYR/PYL3 -----
HvPYR/PYL4 -----
HvPYR/PYL1 LEQ-- 205

Supplemental Figure S1A. Amino acid sequence alignment of the Arabidopsis PYR1/RCAR11 protein with putative barley PYR/PYL orthologous proteins. The alignment was performed with the ClustalW2 program at the EBI web server (http://www.ebi.ac.uk/Tools/msa/clustalw2/ using the default settings. “Gate” and “latch” regions are shaded in yellow. Residues in contact with ABA hormone are indicated in red and bold, according to the PYL2 crystal structure of Melcher *et al.* (2009). * indicates fully conserved residues; : (colon) indicates conservation between groups of strongly similar properties, . (period) indicates conservation between groups of weakly similar properties.

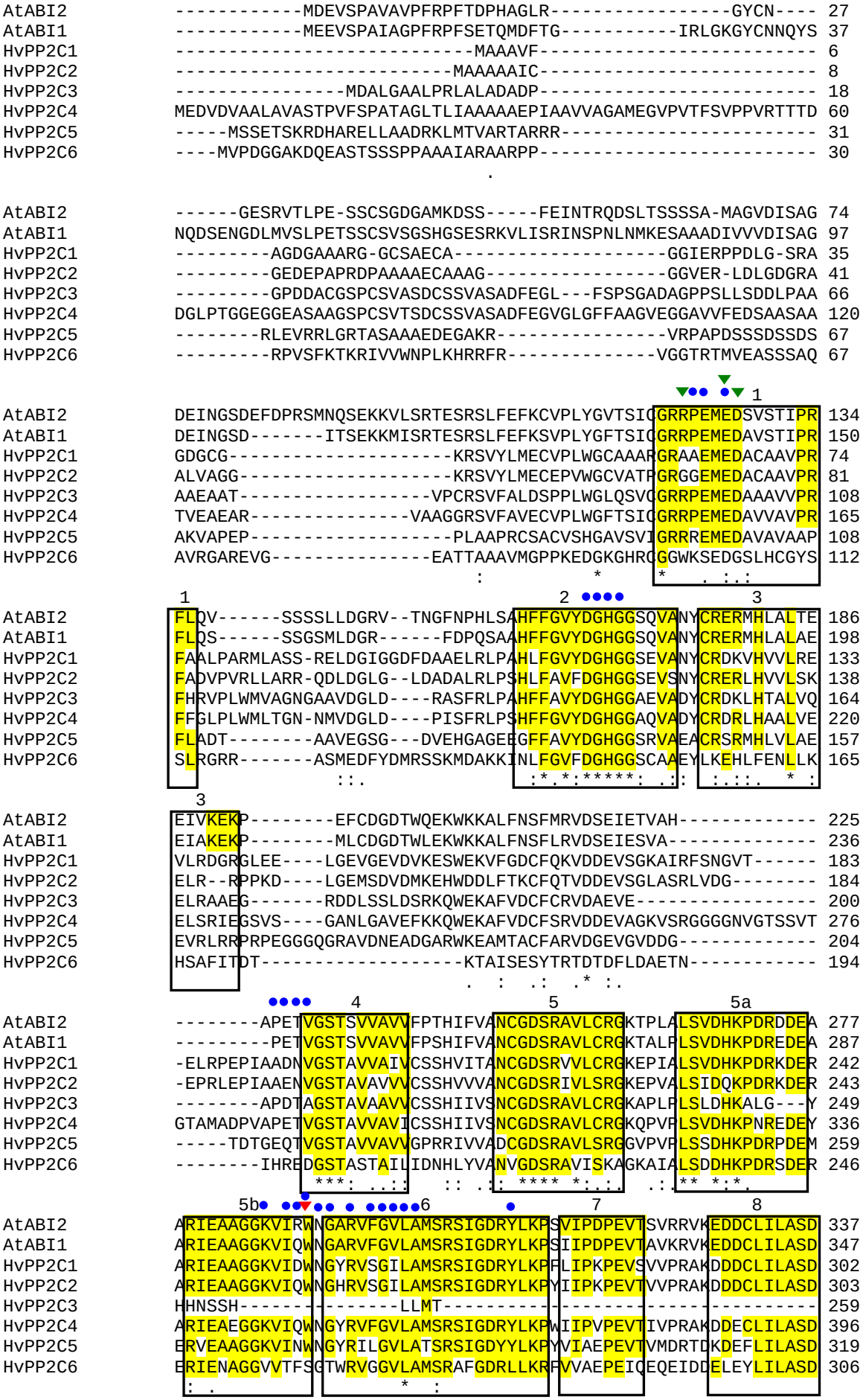
AtABI2 ----------MDEVSPAVAVPFRPFTDPHAGLR----------GYCN---- 27
AtABI1 ----------MEEVSPAIAGPFRPFSETQMDFTG----------IRLGKGYCNNQYS 37
HvPP2C1 ----------MAAAVF---------- 6
HvPP2C2 ----------MAAAAAIC---------- 8
HvPP2C3 ----------MDALGAALPRLALADADP---------- 18
HvPP2C4 MEDVDVAALAVASTPVFSPATAGLTLIAAAAAEPIAAVVAGAMEGVPVTFSVPPVRTTTD 60
HvPP2C5 -----MSSETSKRDHARELLAADRKLMTVARTARRR---------- 31
HvPP2C6 ----MVPDGGAKDQEASTSSSPPAAAIARAARPP---------- 30
AtABI2 ------GESRVTLPE-SSCSGDGAMKDSS-----FEINTRQDSLTSSSSA-MAGVDISAG 74
AtABI1 NQDSENGDLMVSLPETSSCSVSGSHGSESRKVLISRINSPNLNMKESAAADIVVVDISAG 97
HvPP2C1 ---------AGDGAAARG-GCSAECA----------GGIERPPDLG-SRA 35
HvPP2C2 ---------GEDEPAPRDPAAAAECAAAG----------GGVER-LDLGDGRA 41
HvPP2C3 ---------GPDDACGSPCSVASDCSSVASADFEGL---FSPSGADAGPPSLLSDDLPAA 66
HvPP2C4 DGLPTGGEGGEASAAGSPCSVTSDCSSVASADFEGVGLGFFAAGVEGGAVVFEDSAASAA 120
HvPP2C5 --------RLEVRRLGRTASAAAEDEGAKR----------VRPAPDSSSDSSDS 67
HvPP2C6 ---------RPVSFKTKRIVVWNPLKHRRFR----------VGGTRTMVEASSSAQ 67
1
AtABI2 DEINGSDEFDPRSMNQSEKKVLSRTESRSLFEFKCVPLYGVTSIGGRRPEMEDSVSTIPR 134
AtABI1 DEINGSD-------ITSEKKMISRTESRSLFEFKSVPLYGFTSIGGRRPEMEDAVSTIPR 150
HvPP2C1 GDGCG----------KRSVYLMECVPLWGCAAARGRAAEMEDACAAVPR 74
HvPP2C2 ALVAGG----------KRSVYLMECEPVWGCVATPGRGGEMEDACAAVPR 81
HvPP2C3 AAEAAT----------VPCRSVFALDSPPLWGLQSVCGRRPEMEDAAAVVPR 108
HvPP2C4 TVEAEAR----------VAAGGRSVFAVECVPLWGFTSICGRRPEMEDAVVAVPR 165
HvPP2C5 AKVAPEP----------PLAAPRCSACVSHGAVSVIGRRREMEDAVAVAAP 108
HvPP2C6 AVRGAREVG----------EATTAAAVMGPPKEDGKGHRCGGWKSEDGSLHCGYS 112
1 2 3
AtABI2 FLQV------SSSSLLDGRV--TNGFNPHLSAHFFGVYDGHGGSQVANYCRERMHLALTE 186
AtABI1 FLQS------SSGSMLDGR------FDPQSAAHFFGVYDGHGGSQVANYCRERMHLALAE 198
HvPP2C1 FAALPARMLASS-RELDGIGGDFDAAELRLPAHLFGVYDGHGGSEVANYCRDKVHVVLRE 133
HvPP2C2 FADVPVRLLARR-QDLDGLG--LDADALRLPSHLFAVFDGHGGSEVSNYCRERLHVVLSK 138
HvPP2C3 FHRVPLWMVAGNGAAVDGLD----RASFRLPAHFFAVYDGHGGAEVADYCRDKLHTALVQ 164
HvPP2C4 FFGLPLWMLTGN-NMVDGLD----PISFRLPSHFFGVYDGHGGAQVADYCRDRLHAALVE 220
HvPP2C5 FLADT--------AAVEGSG---DVEHGAGEEGFFAVYDGHGGSRVAEACRSRMHLVLAE 157
HvPP2C6 SLRGRR-------ASMEDFYDMRSSKMDAKKINLFGVFDGHGGSCAAEYLKEHLFENLLK 165
3
AtABI2 EIVKEKP--------EFCDGDTWQEKWKKALFNSFMRVDSEIETVAH---------- 225
AtABI1 EIAKEKP--------MLCDGDTWLEKWKKALFNSFLRVDSEIESVA---------- 236
HvPP2C1 VLRDGRGLEE----LGEVGEVDVKESWEKVFGDCFQKVDDEVSGKAIRFSNGVT------ 183
HvPP2C2 ELR--RPPKD----LGEMSDVDMKEHWDDLFTKCFQTVDDEVSGLASRLVDG-------- 184
HvPP2C3 ELRAAEG-------RDDLSSLDSRKQWEKAFVDCFCRVDAEVE---------- 200
HvPP2C4 ELSRIEGSVS----GANLGAVEFKKQWEKAFVDCFSRVDDEVAGKVSRGGGGNVGTSSVT 276
HvPP2C5 EVRLRRPRPEGGGQGRAVDNEADGARWKEAMTACFARVDGEVGVDDG---------- 204
HvPP2C6 HSAFITDT----------KTAISESYTRTDTDFLDAETN---------- 194
4 5 5a
AtABI2 --------APETVGSTSVVAVVFPTHIFVANCGDSRAVLCRGKTPLALSVDHKPDRDDEA 277
AtABI1 ---------PETVGSTSVVAVVFPSHIFVANCGDSRAVLCRGKTALPLSVDHKPDREDEA 287
HvPP2C1 -ELRPEPIAADNVGSTAVVAIVCSSHVITANCGDSRVVLCRGKEPIALSVDHKPDRKDER 242
HvPP2C2 -EPRLEPIAAENVGSTAVAVVVCSSHVVVANCGDSRIVLSRGKEPVALSIDQKPDRKDER 243
HvPP2C3 --------APDTAGSTAVAAVVCSSHIIVSNCGDSRAVLCRGKAPLPLSLDHKALG---Y 249
HvPP2C4 GTAMADPVAPETVGSTAVVAVICSSHIIVSNCGDSRAVLCRGKQPVPLSVDHKPNREDEY 336
HvPP2C5 -----TDTGEQTVGSTAVVAVVGPRRIVVADCGDSRAVLSRGGVPVPLSSDHKPDRPDEM 259
HvPP2C6 --------IHREDGSTASTAILIDNHLYVANVGDSRAVISKAGKAIALSDDHKPDRSDER 246
5b 6 7 8
AtABI2 ARIEAAGGKVIRWNGARVFGVLAMSRSIGDRYLKPSVIPDPEVTSVRRVKEDDCLILASD 337
AtABI1 ARIEAAGGKVIQWNGARVFGVLAMSRSIGDRYLKPSIIPDPEVTAVKRVKEDDCLILASD 347
HvPP2C1 ARIEAAGGKVIDWNGYRVSGILAMSRSIGDRYLKPFLIPKPEVSVVPRAKDDDCLILASD 302
HvPP2C2 ARIEAAGGKVIQWNGHRVSGILAMSRSIGDRYLKPYIIPKPEVTVVPRAKDDDCLILASD 303
HvPP2C3 HHNSSH----------LLMT---------- 259
HvPP2C4 ARIEAEGGKVIQWNGYRVFGVLAMSRSIGDRYLKPWIIPVPEVTIVPRAKDDECLILASD 396
HvPP2C5 ERVEAAGGKVINWNGYRILGVLATSRSIGDYYLKPYVIAEPEVTVMDRTDKDEFLILASD 319
HvPP2C6 ERIENAGGVVTFSGTWRVGGVLAMSRAFGDRLLKRFVVAEPEIQEQEIDDELEYLILASD 306

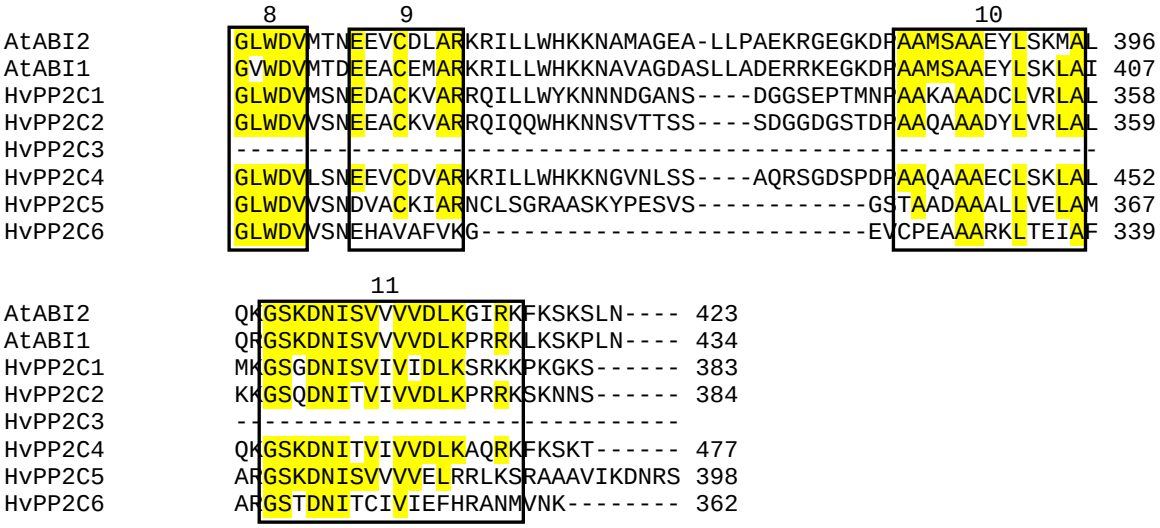

Supplemental Figure S1B. Amino acid sequence alignment of barley and Arabidopsis type-2C protein phosphatases. The Arabidopsis ABI1, ABI2 and the six members from barley were aligned with ClustalW2 program at the EBI web server (http://www.ebi.ac.uk/Tools/msa/clustalw2/ using the default settings. The eleven conserved motifs found in the PP2C family are boxed and numbers are indicated above each region. Conserved amino acids are shaded in yellow. * indicates fully conserved residues; : (colon) indicates conservation between groups of strongly similar properties, . (period) indicates conservation between groups of weakly similar properties. The conserved W residue involved in ABA binding is marked with a red triangle; residues involved in binding to PYR/RCARs are marked with blue circles. Phosphatase sites are indicated by green triangles. Functional residues are based on studies by Melcher *et al*., (2009) and Santiago *et al.*, (2012).

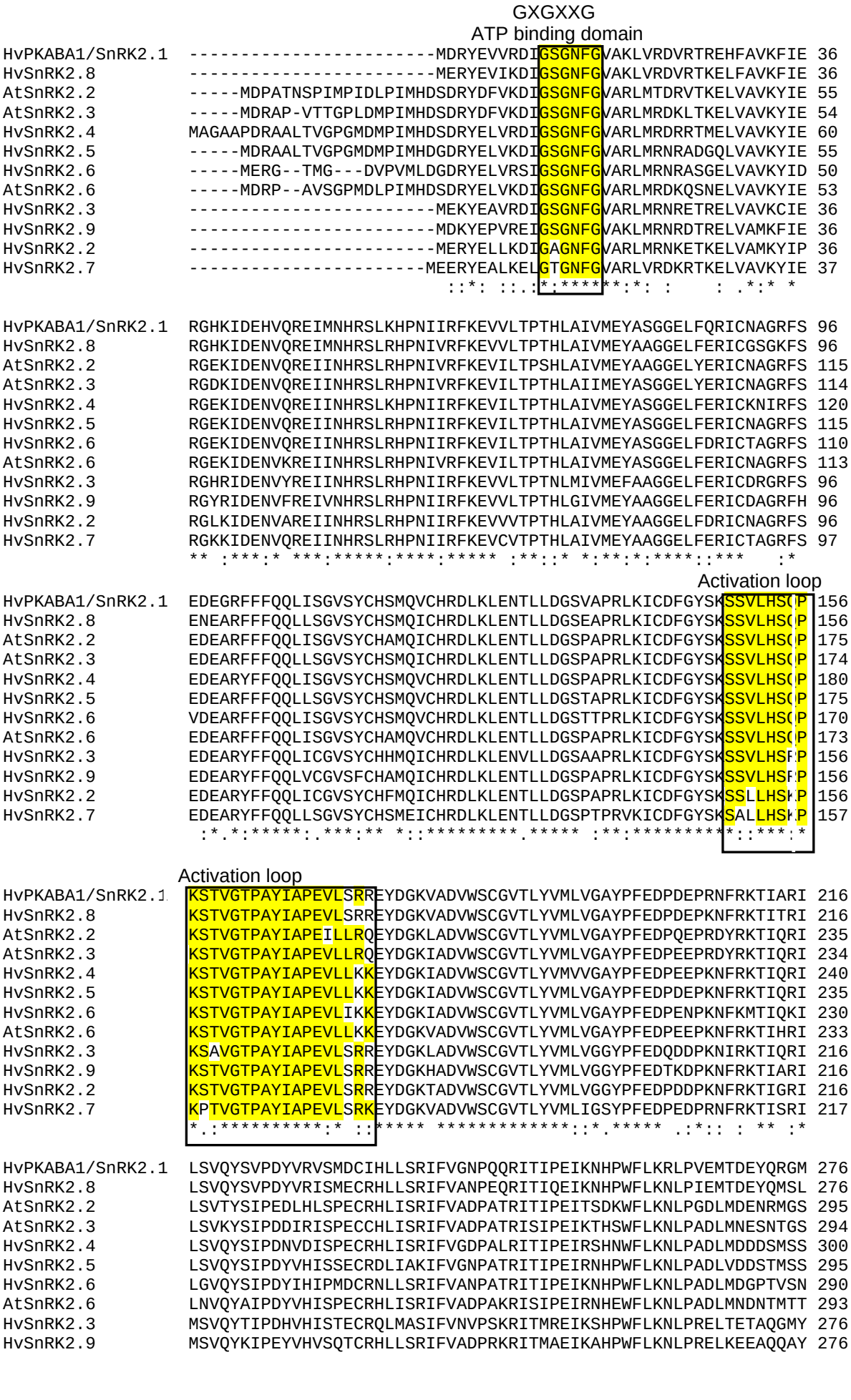
GXGXXG
ATP binding domain
Activation loop
Activation loop

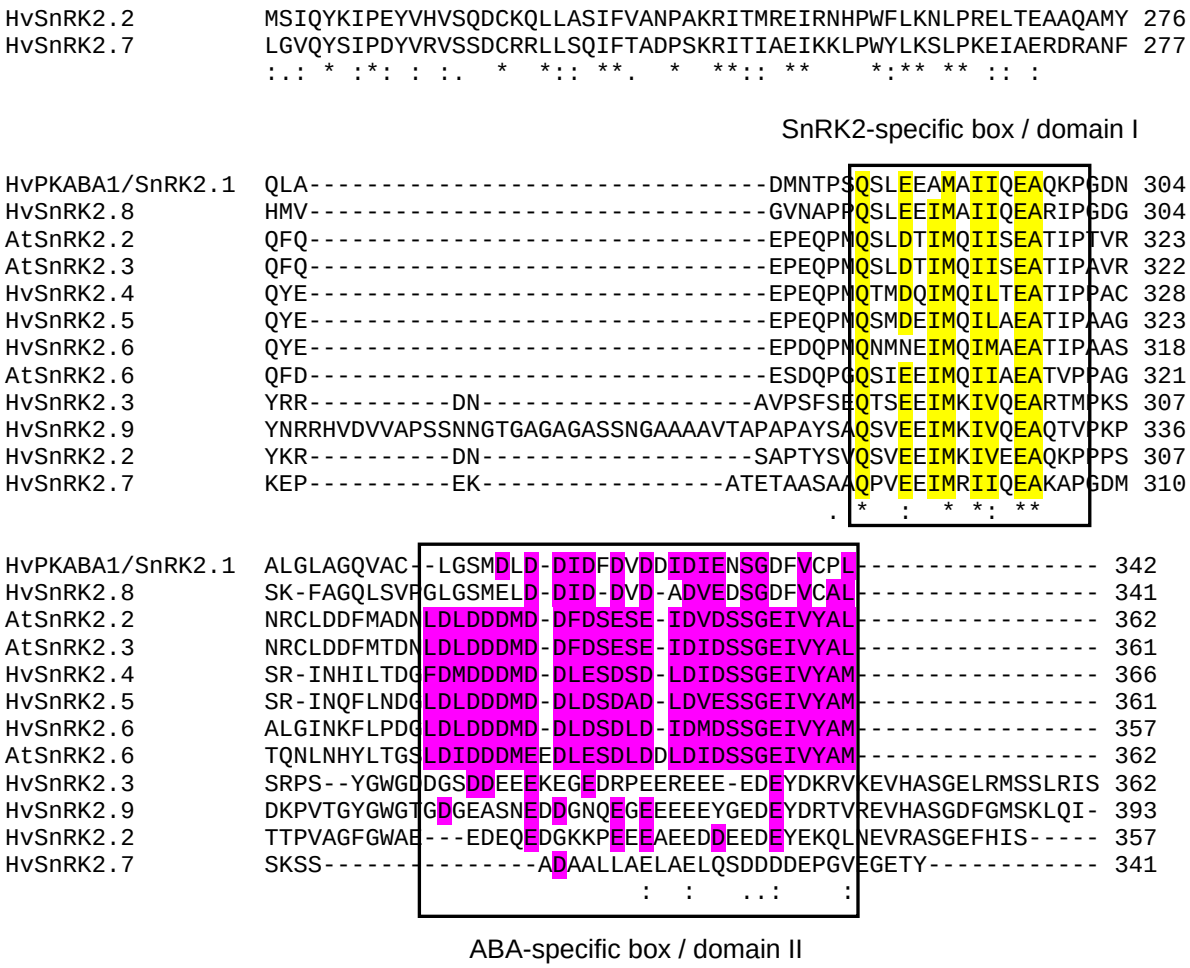

Supplemental Figure S1C. Amino acid sequence alignment of the Arabidopsis SnRK2.2, 2.3 and 2.6 proteins with barley SnRK2 orthologous proteins. The alignment was performed with the ClustalW2 program at the EBI web server (http://www.ebi.ac.uk/Tools/msa/clustalw2/ using the default settings. ATP binding domain, activation loop and C-terminal conserved regions are boxed with conserved amino acids shaded yellow. Conserved residues belonging to the Asp-rich domain of one group of kinases are shaded magenta. * indicates fully conserved residues; : (colon) indicates conservation between groups of strongly similar properties, . (period) indicates conservation between groups of weakly similar properties. Functional domains are noted according to Yoshida *et al*. (2006).

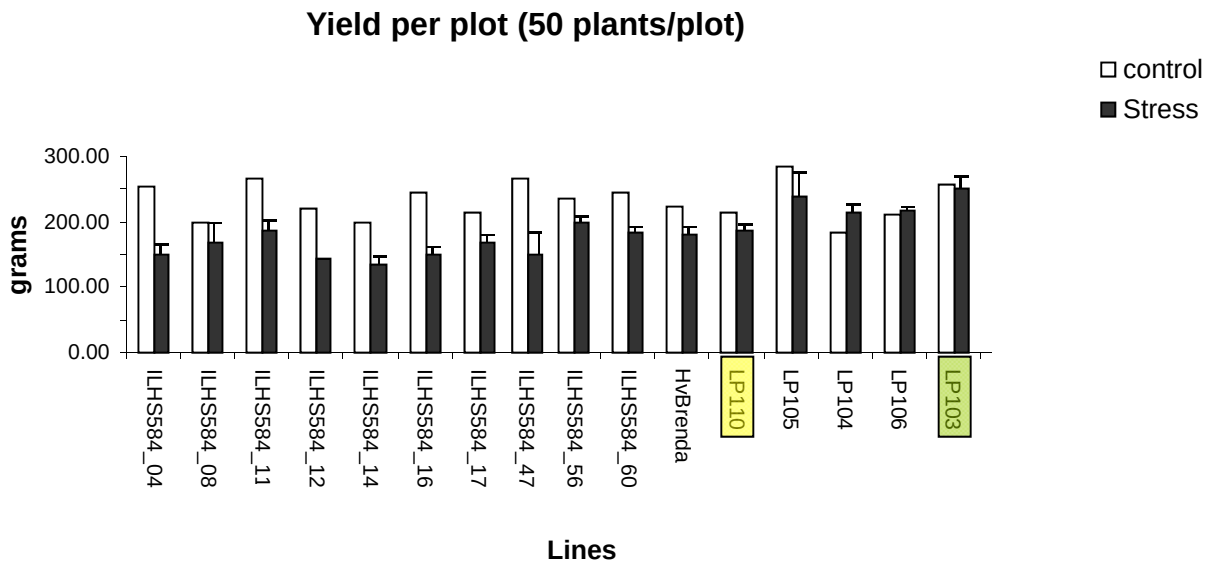

Supplemental Figure S2. Yield data obtained from field screening with 16 selected barley lines. From the breeding panel, stay-green (LP103) and senescing genotype (LP110) are selected, which are indicated by coloured boxes. Bars represent mean values from 10 replicate plots per genotype.

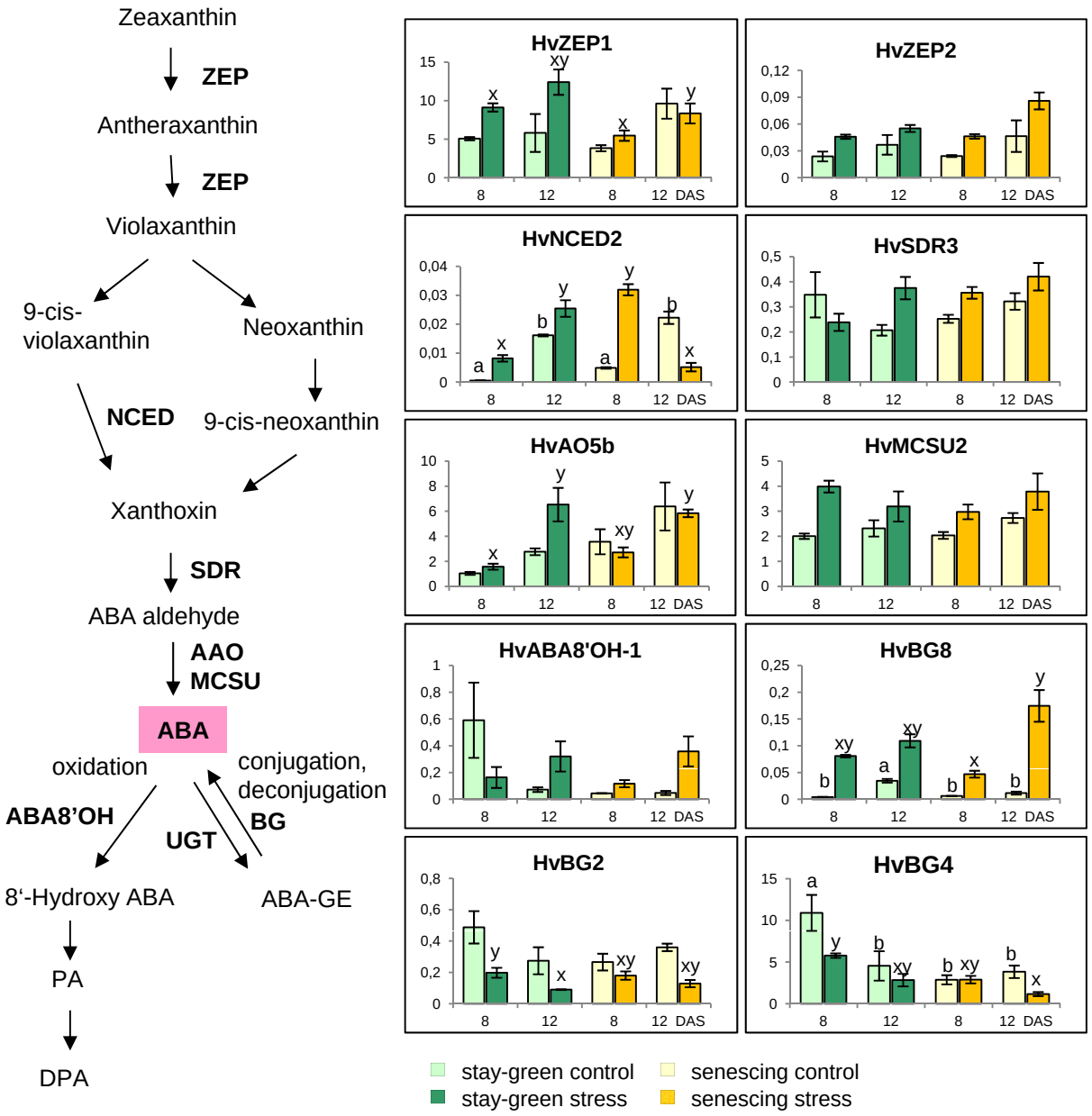

Supplemental Figure S3. Differential expression of putative ABA biosynthesis, degradation and deconjugation genes in two barley contrasting genotypes under terminal drought stress analyzed by qRT-PCR in flag leaves at 8 and 12 days after stress (DAS). The graphs show mean values from two replicates of qRT-PCR-experiments from biological independent material (n=2) with an additional two technical replications. Relative mRNA levels to reference gene HZ42K12 are shown by colour-coded bars (mean ± SD). Statistical significant differences among genotypes and a given treatment have been calculated using one-way ANOVA at $\alpha = 0.05$ with Tukey post-hoc test. Letters a, b and x, y represent statistical differences under control and stress conditions, respectively. The significance of differences between control and stress was determined using two-way ANNOVA with * $p \leq 0.05$ and ** $p \leq 0.001$. Details are given in Supplemental Table S4.

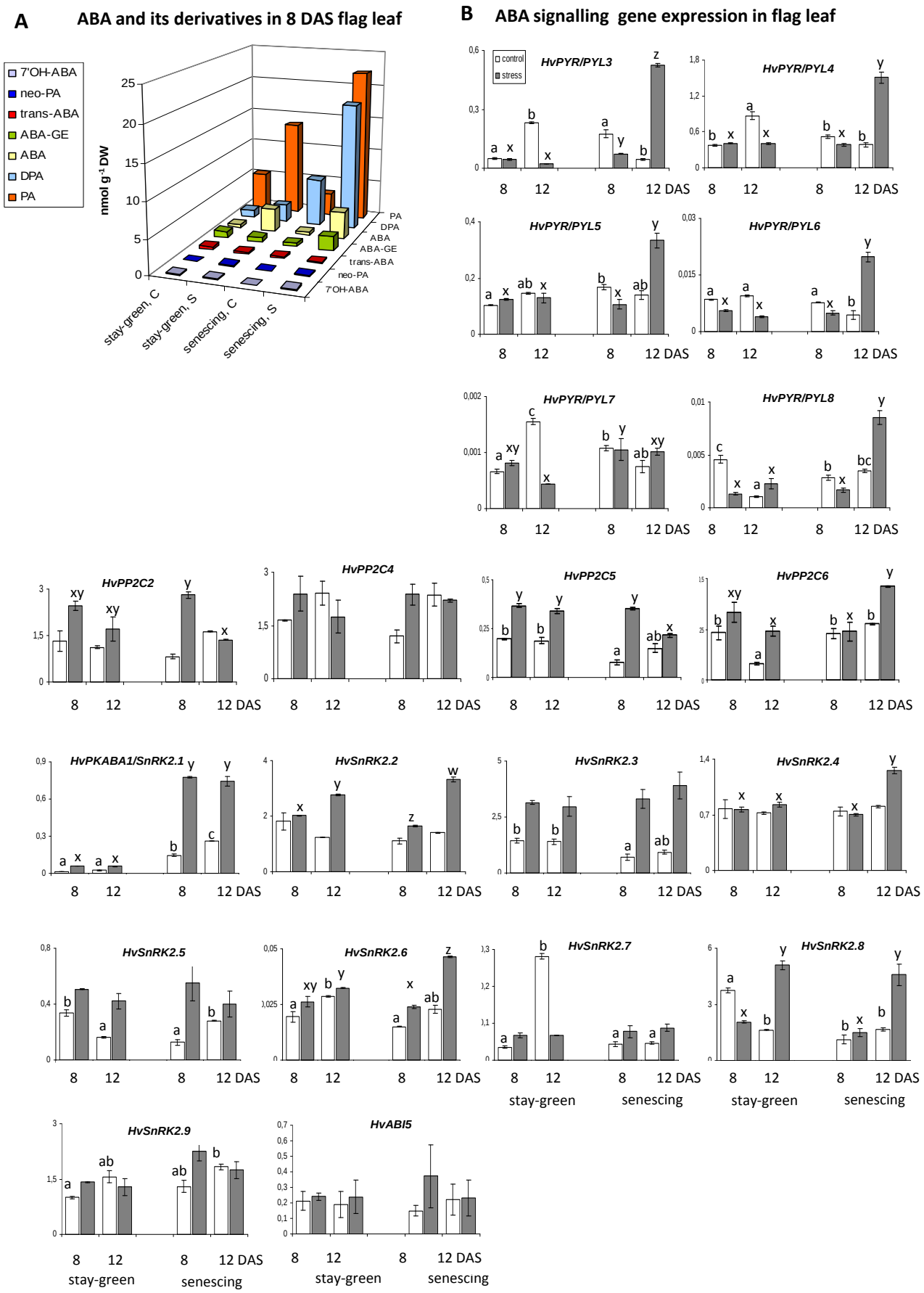
A
ABA and its derivatives in 8 DAS flag leaf
7'OH-ABA
neo-PA
trans-ABA
ABA-GE
ABA
DPA
PA
nmol g-1 DW
stay-green, C
stay-green, S
senescing, C
senescing, S
B
ABA signalling gene expression in flag leaf
control
stress
HvPYR/PYL3
HvPYR/PYL4
HvPYR/PYL5
HvPYR/PYL6
HvPYR/PYL7
HvPYR/PYL8
HvPP2C2
HvPP2C4
HvPP2C5
HvPP2C6
HvPKABA1/SnRK2.1
HvSnRK2.2
HvSnRK2.3
HvSnRK2.4
HvSnRK2.5
HvSnRK2.6
HvSnRK2.7
HvSnRK2.8
HvSnRK2.9
HvABI5
8
12
12 DAS
stay-green
senescing

Supplemental Figure S4. ABA, ABA metabolites and differential expression of putative ABA signaling genes in two barley contrasting genotypes under terminal drought stress. A: Levels of ABA and ABA metabolites in flag leaves and seeds at 8 days after stress (DAS) under control and stress conditions. ABA, *cis*-abscisic acid; PA, phaseic acid; DPA, dihydrophaseic acid; ABA-GE, ABA glucose ester; *neo*-PA, *neo*-phaseic acid; 7'OH-ABA, 7'-Hydroxy-ABA; t-ABA, *trans*-ABA.; DW, dry weight. B: Differentially expressed genes in flag leaves at 8 and 12 DAS. The graphs show mean values from two replicates of qRT-PCR-experiments from biological independent material (n=2) with an additional two technical replications. Relative mRNA levels to reference gene HZ42K12 are shown by white and grey bars (mean ± SD). Days after stress imposition (DAS) are shown on the x-axis.

Statistical analysis was carried out across genotypes for a given treatment using one-way ANOVA at $\alpha = 0.05$ with Tukey post-hoc test Letters a, b, c and x, y, z represent statistical differences under control and stress conditions, respectively. Bars with similar or no letters indicate no statistical difference among genotypes under a given treatment. The significance of differences between control and stress was determined using two-way ANNOVA with * $p \leq 0.05$ and ** $p \leq 0.001$. Details are given in Supplemental Table S4.

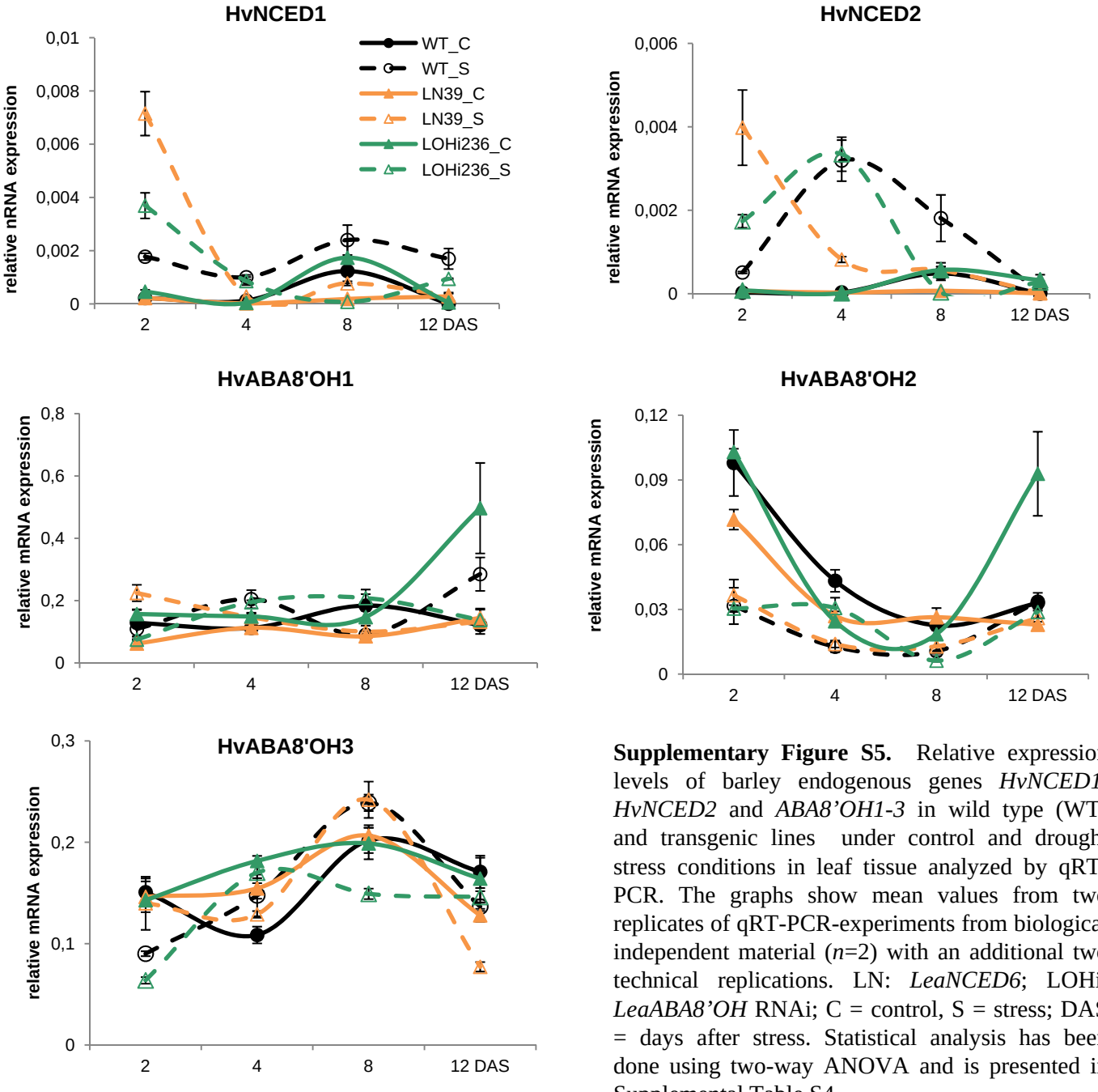

Supplementary Figure S5. Relative expression levels of barley endogenous genes *HvNCED1*, *HvNCED2* and *ABA8'OH1-3* in wild type (WT) and transgenic lines under control and drought stress conditions in leaf tissue analyzed by qRT-PCR. The graphs show mean values from two replicates of qRT-PCR-experiments from biological independent material (*n*=2) with an additional two technical replications. LN: *LeaNCED6*; LOHi: *LeaABA8'OH* RNAi; C = control, S = stress; DAS = days after stress. Statistical analysis has been done using two-way ANOVA and is presented in Supplemental Table S4.

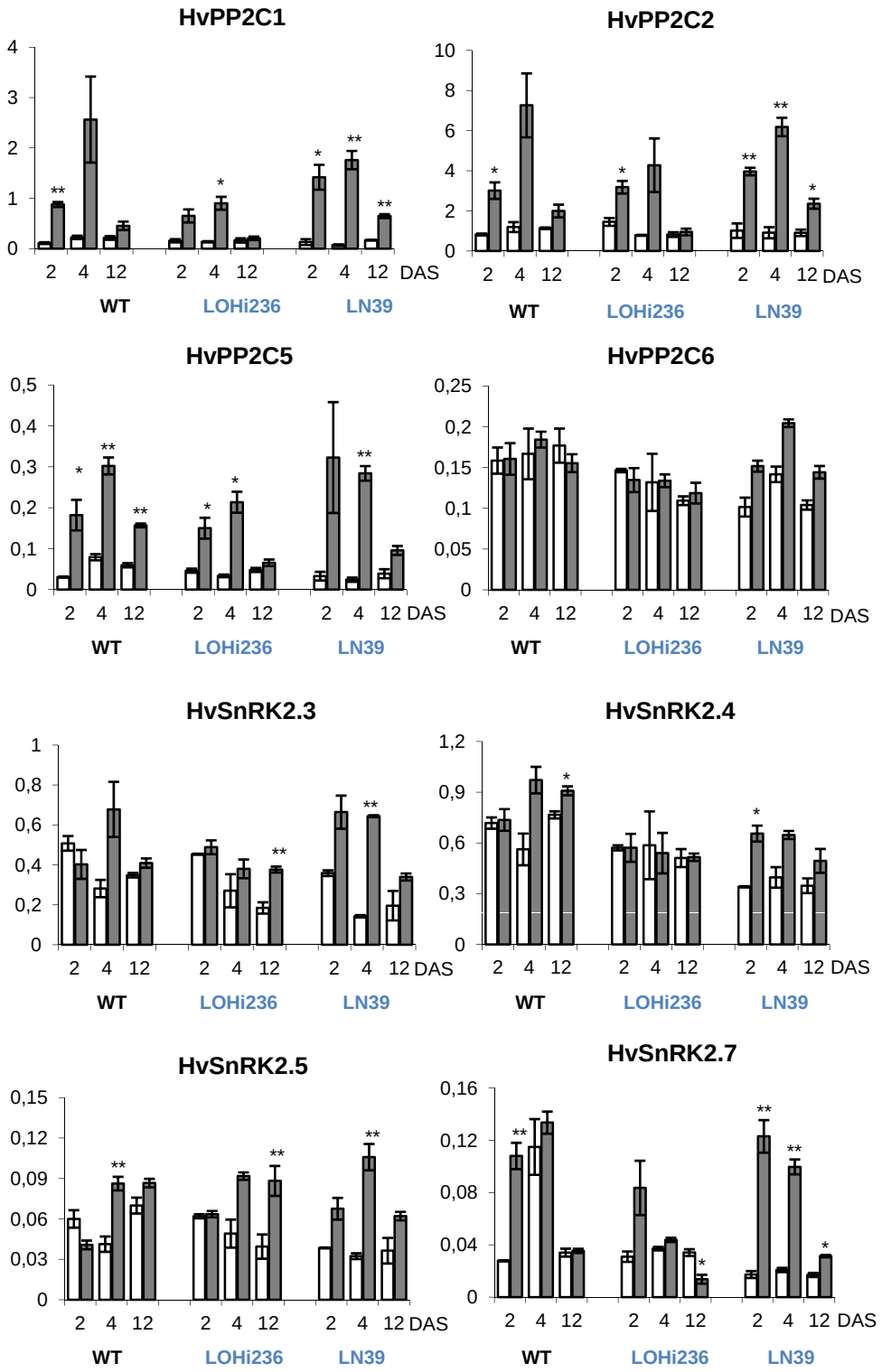

Supplemental Figure S6. Differential expression of putative ABA signaling genes in barley wild type (WT) and transgenic plants under terminal drought stress analyzed by qRT-PCR. Differentially expressed genes in flag leaves which experienced different duration of stress (2, 4 and 12 days after stress imposition, DAS). LOHi236: RNAi line *LeaABA8'OH*, LN39: *LeaNCED6* overexpression. The graphs show mean values from two replicates of qRT-PCR-experiments from biological independent material (n=2) with an additional two technical replications. Relative mRNA levels to reference gene HZ42K12 are shown by white and grey bars (mean ± SD). The significance of differences was determined using two-way ANNOVA with * $p \leq 0.05$ and ** $p \leq 0.001$. Statistical significant differences across genotypes was calculated using one-way ANOVA. Further details are given in Supplemental Table S4.

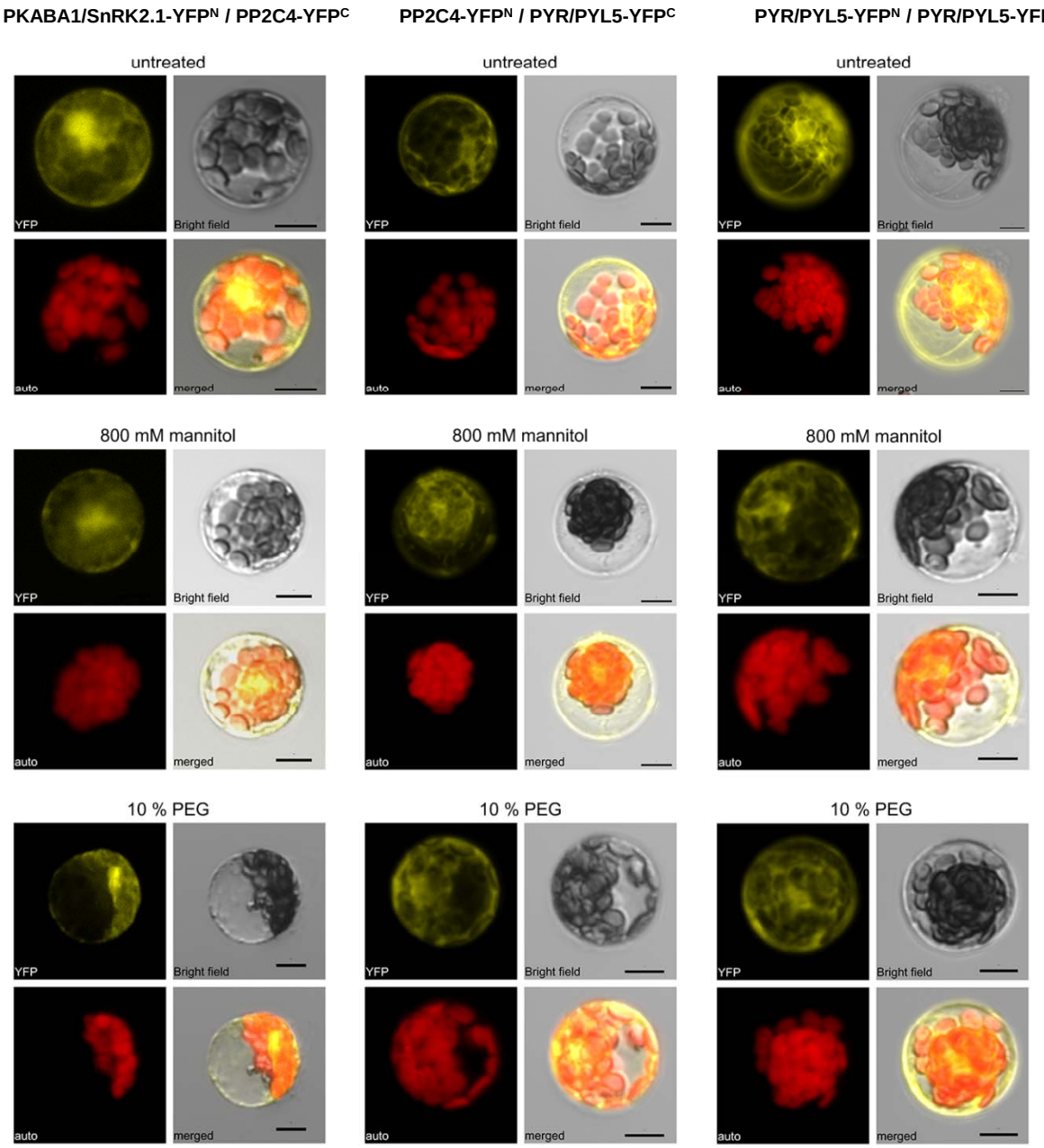

Supplemental Figure S7. Interaction of ABA receptor components using different stress treatments analyzed by BiFC. Pairs of PP2C4-YFP^N / PYR/PYL5-YFP^C , PYR/PYL5-YFP^N / PYR/PYL5-YFP^C and PKABA1/SnRK2.1-YFP^N / PP2C4-YFP^C were transformed into Arabidopsis protoplasts. Fluorescence images were taken 1 d after transformation. The pictures are YFP, bright field, autofluorescence (auto) and merged images, scale bar = 10 µm.

Supplemental Table S1: List of genes putatively involved in ABA signalling/biosynthesis and primer sequences used for qRT-PCR.

Receptor/ Transcription factor/Enzyme	***Gene***	***Forward primer***	***Reverse primer***
PYR/PYL	*HvPYR/PYL1*	AGGCGATCACCGGCTAAGGAAC	GGCCGCCCATCAATACTCTGTG
	HvPYR/PYL2	AGGCCATGGGACGAGCACACTA	AACCGGCGCACGTACTCCATCT
	HvPYR/PYL3	GTTTCTTCGGCGCGTGAGCAT	TTGGACAAGCAGGGAGGAGAGG
	HvPYR/PYL4	CCCCCTCCGGTCAACTCTCG	CCACCACCACCACCACGGATTT
	HvPYR/PYL5	CCGCCGGCAGAATAACGAC	CCCTCCCGAGAAAAAGCAAAGA
	HvPYR/PYL6	GAGGGCAACACCGAGGAGGACA	CGATGGCGGCGAGTTTCTGG
	HvPYR/PYL7	CCGCAGGCGTACAAGCACT	CCGACACGACCCGCACCTC
	HvPYR/PYL8	CGTTCTTGTGCGTGTGGTGATG	CGCCCCGGGAAGGTGTGG
Snf1 related protein kinases	*HvPKABA1/SnRK2.1*	GCAGAAACCGGGCGATAACG	GCTCCCCAGGCAGGCAACC
	HvSnRK2.2	ACAACAGCGCCCCAACCTACTC	CTCCGCCCACCCGAAACC
	HvSnRK2.3	GGGATAACGCCGTGCCTTCTT	GTCGTCGCCCCAACCATAGC
	HvSnRK2.4	TTGTTGGGGATCCTGCTTTGAG	GATCGGCGGGGAGGTTCTTTA
	HvSnRK2.5	ATCCCGGCGGCTGGTTCTC	CAAGGTCGTCCATGTCGTCGTC
	HvSnRK2.6	CTTGCAGCCAGCTACGGTGAG	CTGAGAGCGGAACGGGTGAAAC
	HvSnRK2.7	GCTGCGTGCCTGCTTCGTA	CGCTTCGTGGCCTTATTGTTG
	HvSnRK2.8	GCGCCCCGGCTCAAGATA	AAGGACCTCGGGGGCAATGTAG
	HvSnRK2.9	GAGGGGGAGGAGGAGGAGGAGT	CGGCGCCATGTGGTGAGAAG
Protein phosphatases 2C	*HvPP2C1*	TCGCCAGCAGCCGTGAGC	CCGCCGTGCCCATCGTAGA
	HvPP2C2	GCACGTCGGCAAATCCAGCAGT	TTTCCTCCGGGGTTTCAAGTCG
	HvPP2C3	GGGCGGCAAGGTCATCCAGT	GGGCAACCACCGTCACCTCAG
	HvPP2C4	TGGCCTCTGGGATGTATTGTCG	GAGCCGCTGGATCTGGGGAGTC
	HvPP2C5	ACGCGGCAGCAAGGACAACATC	ATCCCCATCCAGCCAGCCACTC
	HvPP2C6	GATCGTTTGTTGAAGCGGTTTG	CACGTCCCACAGGCCATCACTA
ABI5	*HvABI5*	CCGGTCCCTGTTGCCCCTAAAG	CGCCGCCCATACCGAGTG
9-cis-epoxycarotenoid dioxygenase	*HvNCED1*	CCAGCACTAATCGATTCC	GAGAGTGGTGATGAGTAA
	HvNCED2	(Millar et al., 2006)	(Millar et al., 2006)
		CATGGAAAGAGGAAGTTG	GAAGCAAGTGTGAGCTAAC
		(Millar et al., 2006)	(Millar et al., 2006)
ABA-hydroxylase	*HvABA8'OH1*	AGCACGGACCGTCAAAGTC	TGAGAATGCCTACGTAGTG
		(Millar et al., 2006)	(Millar et al., 2006)
	HvABA8'OH2	GAGATGCTGGTGCTCATC	ACGTCGTCGCTCGATCCAAC
		(Millar et al., 2006)	(Millar et al., 2006)
	HvABA8'OH3	CCGGCGGCAGCGTCTTCT	GTGTTGCCGTCCTGGGTGTCC

Beta-glucosidase	*HvBG2*	GCCGGTGGGAACTCAGCAACAG	GTCGGCAGGTGAGTCGGTAGCA
	HvBG4	CCCGCCGGAGTTCGTCTTC	TCCTCAGCCACAGCACCCTCAT
	HvBG8	CCCCGGCCAGGCGTATTCC	TCCCAGGCTTATTCGTCATCCA
Zeaxanthin epoxidase	*HvZEP1*	GCGAGAGGCGGGGGAGAAGT	TGGTGACAAGGGGTGGCTGAAG
	HvZEP2	CTTCCTGGCTCGTCGGTTCGTC	GCTGGGAGTGGAGGGCGTGTAA
Short-chain dehydrogenase	*HvSDR3*	GCCGCAGCGTCCCCTCTC	ACAACAAGCGCCCAGTCAGTGC
Aldehyde oxidase	*HvAO5b*	TTGGCGTTGTGATTGCTGAGAC	AAAACGGGGGAGGATGGAAGTA
Reference gene	*HZ42K12*	TTACCCTCCTCTTGGTCGTTTTG	TCTTCTTGATGGCAGCCTTGG

Supplemental Table S2. Levels of ABA, ABA metabolites and other hormones in flag leaf and seeds under control and stress conditions at 8 days after stress impositon (DAS).

Hormone levels are given in ng g^{-1} dry weight including standard deviation (SD). [1] Only one of the two biological replicates gave a detectable value, thus no SD was calculated. n. d. not detected. Asterisks in brackets indicate statistical significant differences (Student's *t*-test) between control and stress with * $p \leq 0.05$. Two-way ANNOVA statistics is presented in Supplemental Table S3.

Substance	***Short name***	***Stay-green Control Flag leaf***	***Stress Flag leaf***	***Senescing Control Flag leaf***	***Stress Flag leaf***
cis-Abscisic acid	ABA	115 ± 0.1	870 ± 335.4	110 ± 21.6	1054 ± 613.8
Abscisic acid glucose ester	ABA-GE	402[1]	292 ± 11.6	189[1]	858 ± 171.1 (*)
Phaseic acid	PA	1506 ± 131.5	3812 ± 227.7 (*)	911 ± 452.4	6212 ± 2240.1
Dihydrophaseic acid	DPA	310 ± 52.5	689 ± 205.7	1924 ± 1105.8	5198 ± 724
7'-Hydroxy-abscisic acid	7'-OH-ABA	39[1]	55.5 ± 5.5	n. d.	56 ± 26
neo-Phaseic acid	*neo*-PA	15[1]	44 ± 30	21[1]	42.5 ± 4.5
trans-Abscisic acid	*trans*-ABA	110[1]	52 ± 8	67[1]	30.5 ± 3.5
cis-Zeatin-O-glucoside	c-ZOG	267.5 ± 10.5	274 ± 34	354.5 ± 9.5	388 ± 17
trans-Zeatin	t-Z	n. d.	n. d.	n. d.	n. d.
trans-Zeatin riboside	t-ZR	7.5 ± 0.5	5 ± 0	6 ± 2	8 ± 2
Indole-3-acetic acid	IAA	21 ± 6	31.5 ± 9.5	19[1]	29 ± 5
N-(Indole-3-yl-acetyl)-aspartic acid	IAA-Asp	n. d.	n. d.	n. d.	n. d.
Gibberellin 4	GA4	n. d.	n. d.	n. d.	n. d.
Gibberellin 34	GA34	n. d.	n. d.	n. d.	n. d.

Supplemental table S3. Statistical significant differences in expression of ABA biosynthesis and signalling genes between genotypes, ABA metabolites and physiological traits

Two-way ANOVA performed to identify the signified difference between accessions (stay-green versus senescing lines) and condition (control versus drought stress) with P values of the f-test. at α = 0.05 yellow colour and 0.001 with pink colour.

	Pr(>F)		
	accession	condition	accession: condition (a:c)
PA	0,48	0,03	0,26

	Pr(>F)		
	accession	condition	accession:condition
DPA	0,01	0,05	0,10

	Pr(>F)		
	accession	condition	accession:condition
ABA.GE	0,20	0,16	0,12

	Pr(>F)		
	accession	condition	accession:condition
ABA	0,89	0,10	0,44

	4DAS		
	accession	condition	accession:condition
A	0,00	0,00	0,00
E	0,00	0,00	0,00
gs	0,00	0,00	0,01
WUE	0,00	0,00	0,00

	8DAS		
	accession	condition	accession:condition
A	0,18	0,00	0,00
E	0,00	0,00	0,00
gs	0,19	0,00	0,26
WUE	0,07	0,00	0,00

	Pr(>F)		
	accession	condition	accession:condition
Transpiration	0,00	0,00	0,00

	Pr(>F)		
	accession	condition	accession:condition
stom.conduct	0,19	0,00	0,26

	Pr(>F)		
	accession	condition	accession:condition
Assimilation	0,18	0,00	0,00

	Pr(>F)		
	accession	condition	accession:condition
WUE	0,07	0,00	0,00

	Pr(>F)		
	accession	condition	accession: condition
ABAOH1	0,11	0,29	0,16
AO5b	0,03	0,79	0,28
BG2	0,14	0,02	0,19
BG4	0,00	0,01	0,01
BG8	0,01	0,00	0,01
MCSU2	0,08	0,00	0,07
NCED2	0,00	0,00	0,00
SDR3	0,84	0,95	0,10
ZEP1	0,00	0,00	0,04
ZEP2	0,91	0,00	0,99
PYL3	0,00	0,01	0,01
PYL4	0,03	0,06	0,01
PYL5	0,08	0,12	0,02
PYL6	0,08	0,00	0,99
PYL7	0,04	0,57	0,46
PYL8	0,06	0,00	0,01
PP2C2	0,71	0,00	0,08
PP2C4	0,49	0,03	0,53
PP2C5	0,00	0,00	0,00
PP2C6	0,28	0,23	0,32
SnRK2.1	0,00	0,00	0,00
SnRK2.2	0,03	0,09	0,38
SnRK2.3	0,28	0,00	0,13
SnRK2.4	0,52	0,76	0,82
SnRK2.5	0,27	0,01	0,12
SnRK2.6	0,11	0,01	0,57
SnRK2.7	0,38	0,02	0,89
SnRK2.8	0,00	0,02	0,00
SnRK2.9	0,03	0,01	0,16
ABI5C	0,77	0,31	0,42

Supplemental table S4. Statistical significant differences in expression of ABA biosynthesis and signalling genes between genotypes, ABA metabolites and physiological traits. Two-way ANOVA performed to identify the signified difference between accessions (WT versus transgenic lines) and condition (control versus drought stress) with P values of the f-test. at α = 0.05 yellow colour and 0.001 with pink colour.

	0.5DAS		
	accession	condition	accession: condition
ABA	1,97092E-18	3,26386E-22	1,0542E-21

	2DAS		
	accession	condition	accession:conditi
ABA	5,35331E-10	1,2785E-14	4,4577E-09

	4DAS		
	accession	condition	accession: condition
ABA	1,00728E-06	4,37241E-13	1,8654E-06

	8DAS		
	accession	condition	accession:conditi
ABA	0,0001766	1,81856E-08	7,6583E-05

	12DAS		
	accession	condition	accession: condition
ABA	0,06464358	5,24353E-05	0,00195802

	2DAS		
	accession	condition	accession: condition
HvNCED1	0,000545313	9,16009E-08	0,00046473
HvNCED2	0,01247954	0,000186649	0,01426485
HvOH1	0,4755137	0,6821573	0,05433579
HvOH2	0,5031865	6,53919E-06	0,2353506
HvOH3	0,170472	0,03274808	0,1781575

	8DAS		
	accession	condition	accession: condition
HvNCED1	0,07608875	0,9458097	0,05051297
HvNCED2	0,00237305	0,9861702	0,8511587
HvOH1	0,1868525	0,3812774	0,03742999
HvOH2	0,0182674	0,05378561	0,01776784
HvOH3	0,01252186	0,016088	0,4596926

	Pr(>F)		
	accession	condition	accession: condition
Assimilatio	8,23E-10	5,70E-54	3,00E-17
WUE	1,03E-09	0,009329111	3,03E-09

	4DAS		
	accession	condition	accession: condition
HvNCED1	0,002149847	3,15072E-07	0,01171593
HvNCED2	0,04358301	0,1547288	0,053761
HvOH1	0,08744942	0,8410828	0,1129395
HvOH2	0,1679798	0,000541223	0,9771922
HvOH3	0,01739717	0,5997266	0,03585336

	12DAS		
	accession	condition	accession: condition
HvNCED1	0,09234385	0,3715041	0,07811752
HvNCED2	0,004969074	2,41306E-07	0,00478103
HvOH1	0,1412324	0,003135118	0,3416329
HvOH2	0,2080661	0,003722729	0,00317209
HvOH3	0,01953302	0,9606031	0,1231886

	accession	condition	accession: condition
RWC	0,0004382	0,0000000	0,0029311

	2DAS		
	accession	condition	accession: condition
HvPP2C1	0,04734	0,00012	0,04000
HvPP2C2	0,19426	0,00006	0,17049
HvPP2C4	0,27139	0,00010	0,15355
HvPP2C5	0,38597	0,00894	0,32555
HvPP2C6	0,11499	0,25478	0,12047
PKABA1.SN	0,12430	0,00016	0,05222
PYR.PYL1	0,05162	0,50789	0,02046
PYR.PYL2	0,01641	0,18632	0,69155
PYR.PYL3	0,03983	0,00079	0,04726
PYR.PYL4	0,00187	0,00023	0,01511
PYR.PYL5	0,07522	0,04900	0,16677
PYR.PYL7	0,22068	0,60709	0,45651
PYR.PYL8	0,11549	0,53886	0,16878
PYR.PYL9	0,00020	0,00018	0,00267
SnRK2.3	0,53887	0,10250	0,01638
SnRK2.4	0,00933	0,03290	0,03223
SnRK2.5	0,07640	0,35322	0,00549
SnRK2.7	0,49146	0,00011	0,12618

	4DAS		
	accession	condition	accession: condition
HvPP2C1	0,12813	0,00162	0,17016
HvPP2C2	0,23360	0,00047	0,38787
HvPP2C4	0,01325	0,00006	0,03988
HvPP2C5	0,01542	0,00000	0,11364
HvPP2C6	0,13860	0,14808	0,36052
PKABA1.SN	0,02536	0,00001	0,00827
PYR.PYL1	0,08219	0,15620	0,17172
PYR.PYL2	0,97713	0,00065	0,99157
PYR.PYL3	0,12387	0,00185	0,12451
PYR.PYL4	0,57630	0,01821	0,35276
PYR.PYL5	0,02068	0,01198	0,01693
PYR.PYL7	0,13489	0,09193	0,88274
PYR.PYL8	0,54628	0,01367	0,94371
PYR.PYL9	0,02648	0,00025	0,03743
SnRK2.3	0,17342	0,00115	0,07570
SnRK2.4	0,13814	0,06413	0,19410
SnRK2.5	0,60211	0,00007	0,11118
SnRK2.7	0,00033	0,00470	0,02078

	12DAS		
	accession	condition	accession: condition
HvPP2C1	0,00811	0,00054	0,00957
HvPP2C2	0,01610	0,00230	0,04153
HvPP2C4	0,00327	0,00046	0,00776
HvPP2C5	0,00152	0,00012	0,00727
HvPP2C6	0,01001	0,37224	0,10318
PKABA1.SNF	0,01958	0,00568	0,18582
PYR.PYL1	0,00000	0,07220	0,26329
PYR.PYL2	0,00570	0,00118	0,03165
PYR.PYL3	0,03815	0,00240	0,03655
PYR.PYL4	0,00162	0,00110	0,00679
PYR.PYL5	0,49990	0,82692	0,83354
PYR.PYL7	0,05187	0,19850	0,75694
PYR.PYL8	0,00720	0,00089	0,04534
PYR.PYL9	0,45450	0,03850	0,31101
SnRK2.3	0,03815	0,00374	0,24784
SnRK2.4	0,00017	0,03257	0,25720
SnRK2.5	0,02527	0,00278	0,17667
SnRK2.7	0,00549	0,45058	0,00089